Article

Systematic bone tool production at 1.5 million years ago

https://doi.org/10.1038/s41586-025-08652-5

Received: 5 March 2024

Accepted: 15 January 2025

Published online: 05 March 2025

Open access

Check for updates

Ignacio de la Torre[1]✉, Luc Doyon[2], Alfonso Benito-Calvo[3], Rafael Mora[4], Ipyana Mwakyoma[1], Jackson K. Njau[5,6]✉, Renata F. Peters[7], Angeliki Theodoropoulou[1] & Francesco d'Errico[2,8]

Recent evidence indicates that the emergence of stone tool technology occurred before the appearance of the genus *Homo*[1] and may potentially be traced back deep into the primate evolutionary line[2]. Conversely, osseous technologies are apparently exclusive of later hominins from approximately 2 million years ago (Ma)[3,4], whereas the earliest systematic production of bone tools is currently restricted to European Acheulean sites 400–250 thousand years ago[5,6]. Here we document an assemblage of bone tools shaped by knapping found within a single stratigraphic horizon at Olduvai Gorge dated to 1.5 Ma. Large mammal limb bone fragments, mostly from hippopotamus and elephant, were shaped to produce various tools, including massive elongated implements. Before our discovery, bone artefact production in pre-Middle Stone Age African contexts was widely considered as episodic, expedient and unrepresentative of early *Homo* toolkits. However, our results demonstrate that at the transition between the Oldowan and the early Acheulean, East African hominins developed an original cultural innovation that entailed a transfer and adaptation of knapping skills from stone to bone. By producing technologically and morphologically standardized bone tools, early Acheulean toolmakers unravelled technological repertoires that were previously thought to have appeared routinely more than 1 million years later.

The incorporation of animal resources into the diet of hominins was a milestone in the evolution of our species[7], with recent evidence confirming that, by 2.6 Ma, hominins modified mammal carcases with stone tools to access meat[8]. As a consequence of the encroachment of technology-driven hominins in the carnivore guild, one of the questions that follow is when the utility of animal skeletal elements expanded to include artefact manufacture in addition to their primary role for consumption[4,9]. This innovation entailed specific knowledge—technological and also anatomical—to be transmitted through social learning in parallel with lithic technology, opening opportunities for new flexible adaptations that contributed to shaping the evolution of Pleistocene hominin cultures.

The Lower Pleistocene bone tool evidence is sparse; limb shaft fragments and horn cores were used—but not intentionally shaped by knapping—in digging and termite foraging activities at several southern African sites dated between 2.4 and 0.8 Ma[3,10–13]. At Olduvai Gorge in Tanzania, only a few fossils previously purported as bone tools[14] have stood scrutiny[4,15,16] and include surface finds (that is, out of their original sedimentary context) and isolated specimens dispersed across a stratigraphic interval spanning over 1 million years[14]. Konso in Ethiopia has also yielded some scattered knapped bone artefacts, including the discovery of a bone handaxe found on the surface but attributed to 1.4 Ma deposits[17].

Bone tools shaped by knapping become more frequent in the Eurasian Middle Pleistocene after 500 thousand years ago (ka)[5]. Bone bifaces are found at several sites from the Levant at Revadim Quarry[18], Central Europe at Vértesszőlős[19] and Bilzingsleben[20], and southern Europe at Fontana Ranuccio and Castel di Guido[5], as well as at the Bashiyi Quarry, Chongqing, China[21]. Possible expedient bone shaft fragments bearing one or more edges with flake removal scars on the cortical or the medullar surface, some of which have been interpreted as wedges or intermediate tools, are present in Europe as early as marine isotope stage 9 at Gran Dolina, Spain[22], Schöningen, Germany[23,24], and in Italy[5] at Castel di Guido, Bucobello, La Polledrara di Cecanibbio and Rebibbia-Casal de' Pazzi. In East Asia, similar tools are reported throughout the Pleistocene[25]. Bone tools shaped with techniques such as scraping, grinding and gouging, which allowed the production of diversified and specialized tool types such as spear and arrow points, barbed points, awls and needles, only appear during the Upper Pleistocene in the African Middle Stone Age after 90 ka[26–29] and in Eurasia after 45 ka[30–34].

The sparse nature of the early knapped bone tool record has prevented researchers from identifying behavioural consistencies in their production and use, and establish the role they had in early hominin subsistence and cognition. Here we describe a bone tool assemblage from a single horizon securely dated to 1.5 Ma at Olduvai Gorge Bed II, Tanzania, which precedes other evidence of systematic bone tool production by more than 1 million years and sheds new light on the almost unknown world of early hominin bone technology.

[1]Instituto de Historia, CSIC-Spanish National Research Council, Madrid, Spain. [2]Université de Bordeaux, CNRS UMR5199 PACEA, MCC, Pessac, France. [3]Centro Nacional de Investigación sobre la Evolución Humana (CENIEH), Burgos, Spain. [4]Facultat de Lletres, Universitat Autonoma de Barcelona, Bellaterra, Spain. [5]Department of Earth and Atmospheric Sciences, Indiana University, Bloomington, IN, USA. [6]The Stone Age Institute, Gosport, IN, USA. [7]Institute of Archaeology, University College London, London, UK. [8]SFF Center for Early Sapiens Behaviour (Sapien CE), University of Bergen, Bergen, Norway. ✉e-mail: ignacio.delatorre@csic.es; jknjau@iu.edu

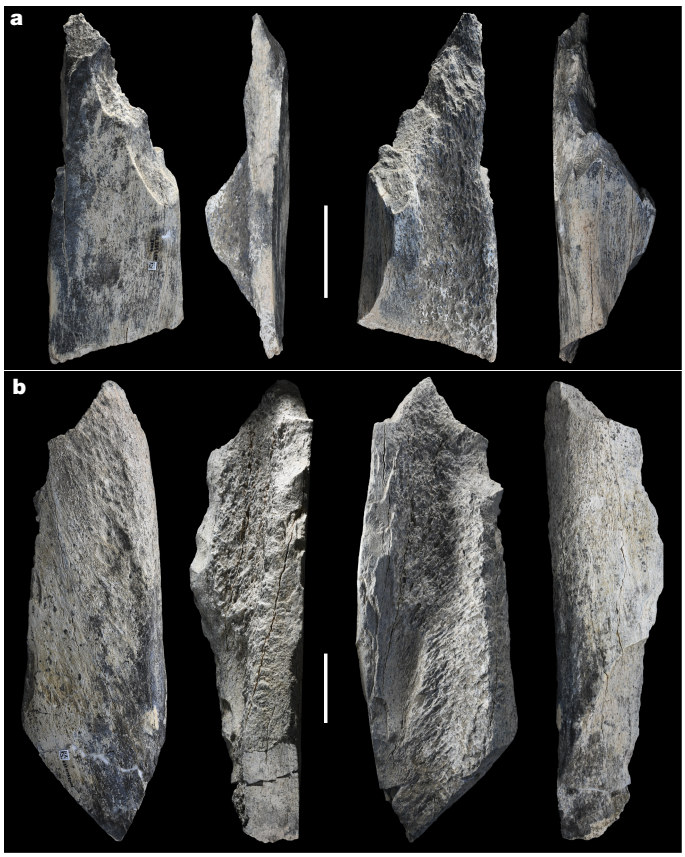

Fig. 1 | Tools made on long bone diaphysis of very large mammals. **a**, Indeterminable taxon larger than two tonnes (accession number T69L20-3009). **b**, Elephant (accession number T79L10-2511). Scale bars, 5 cm. See also Extended Data Fig. 6 and Supplementary Videos 4 and 5.

The T69 Complex archaeological site

The T69 Complex is located in the Frida Leakey Korongo (FLK) West Gully at Olduvai Gorge, in northern Tanzania (Extended Data Fig. 1). This site is positioned in the stratigraphic interval between Middle and Upper Bed II, in which early Acheulean assemblages are reported. Radiometric and chronostratigraphic data firmly position the T69 Complex site at 1.5 Ma (Methods).

The T69 Complex includes seven trenches excavated between 2015 and 2022 (Methods; Supplementary Information Videos 1 and 2). The archaeological assemblage that yielded the bone tools was deposited within interlayering silts and sands indicative of an alluvial plain environment with alternating decantation and water flow facies. It contains over 10,900 stone tools that are 2 cm or longer, mostly made on locally available quartzite, and numerous smaller lithic artefacts (more than 41,000). The lithic assemblage includes cores (n = 747) and split cobbles (n = 50), pounded (n = 273) and retouched (n = 230) tools, flakes (n = 2,804) and flake fragments (n = 8,358), and is attributed to the Acheulean[35] owing to the presence of large cutting stone tools (LCT; n = 37). The assemblage also contains over 9,419 identifiable vertebrate fossils and 13,413 unidentified bone fragments. Abundant fish, crocodile and hippopotamus remains are consistent with lithological data indicating the proximity of water sources. The large mammal assemblage is dominated by bovids and hippopotamus, the latter represented by relatively complete carcasses. Equids, suidae, elephants, rhinoceros and other taxa are also present. *Hippopotamus* is the most abundant genus, and bones frequently exhibit evidence of anthropogenic manipulation, suggesting that hominins were attracted to the T69 Complex area by the availability of hippopotamus carcasses (Methods; Supplementary Data 1).

The bone tool assemblage

The T69 Complex faunal assemblage, including the bone tools, presents an excellent state of preservation that allows documentation of natural and anthropogenic modifications in detail. Taphonomic and morphometric analyses rule out natural processes to account for the modifications recorded on the 27 specimens identified as bone tools (Methods). Several factors are known to cause flake removals on bone that mimic intentional flaking[4], including carnivores gnawing, crocodiles biting, trampling and fracturing to access marrow. Several reasons rule out these factors: carnivore remains amount to less than 1% of the identified specimens. With the exception of two possible tooth marks (Supplementary Data 2), no modifications produced by carnivores are recorded on the T69 Complex bone tools, whereas they are abundant in bone assemblages modified by these agents and yielding fragments bearing flake removals[36,37]. The fresh appearance of the edges of the tools and the rarity of striations attributable to trampling indicate that this process had minimal effect on the state of preservation of the bone artefacts and cannot be the cause for the numerous invasive flake removals present on them. Experimental breakage of large mammal limb bones for marrow extraction, including elephant bones, has demonstrated that flake removal scars resulting from this activity rarely amount to more than four (Extended Data Fig. 4f–h), they are mostly isolated or, when contiguous, rarely exceed three, and they preferentially occur on the ends rather than the lateral sides of the splinters[4,9]. T69 Complex faunal fragments display an average of 2.1 flake scars that occur as isolated removals in 84.3% of the specimens (Extended Data Fig. 4b–d), conforming with a pattern typical of limb bone breaking to access marrow. By contrast, the T69 Complex bone tools exhibit an average of 12.9 flake scars per specimen (Extended Data Fig. 4i–k) and are always arranged contiguously and preferentially—but not exclusively—on their lateral edges.

All 27 bone tools were found in situ during excavation (Supplementary Video 3). Eighteen (66.7%) come from bones attributed to mammals heavier than two tonnes (Fig. 1, Extended Data Fig. 5 and Supplementary Data 2). Among the 16 taxonomically identifiable specimens, eight are from elephant, six are from hippopotamus and two from bovids (Supplementary Data 2). Thus, although the mammal assemblage is dominated by bovids (41.1%), a minimum of 50% of bone tools are made from elephant, which only makes 1.1% of the T69 Complex taxa composition. With the exception of a single proximal portion of a large bovid radius that preserves part of its epiphysis, all tools are exclusively made on limb bone shaft fragments, particularly femora, tibiae and humeri.

The bone tools display morphological, technological and dimensional characters identifying behavioural patterns previously undocumented at early hominin sites. The surface of flake removals is fresh, which is indicative of the short period of subaerial exposure elapsed between bone tool production and burial. All tools made of hippopotamus limb fragments come from bones broken while they were in a nutritive state. For those made of elephant, both fresh and partially weathered bones were used (Supplementary Data 2), which suggests that hominins accessed fresh carcasses but also defleshed bones. The tools are considerably longer than most of the faunal assemblage and fall within the size range of experimentally broken elephant long bones[4] (Extended Data Fig. 4a,e,i). Bone tools made from elephant bones are the largest, ranging between approximately 22 and 38 cm in length, and approximately 8 and 15 cm in width. Tools made from hippo bones are slightly smaller with ranges between approximately 18 and 30 cm in length and approximately 6 and 8 cm in width (Extended Data Fig. 5).

Elephant bone tools bear on average more flake removal scars (μ = 17.3) than those made on hippopotamus bone (μ = 13.3). Among the taxonomically unidentifiable specimens, seven bone tools show sizes and number of flake removal scars that are compatible with those made on elephant or hippopotamus bones. Eight tools are smaller in size and bear on average six flake removal scars. When shaping bone

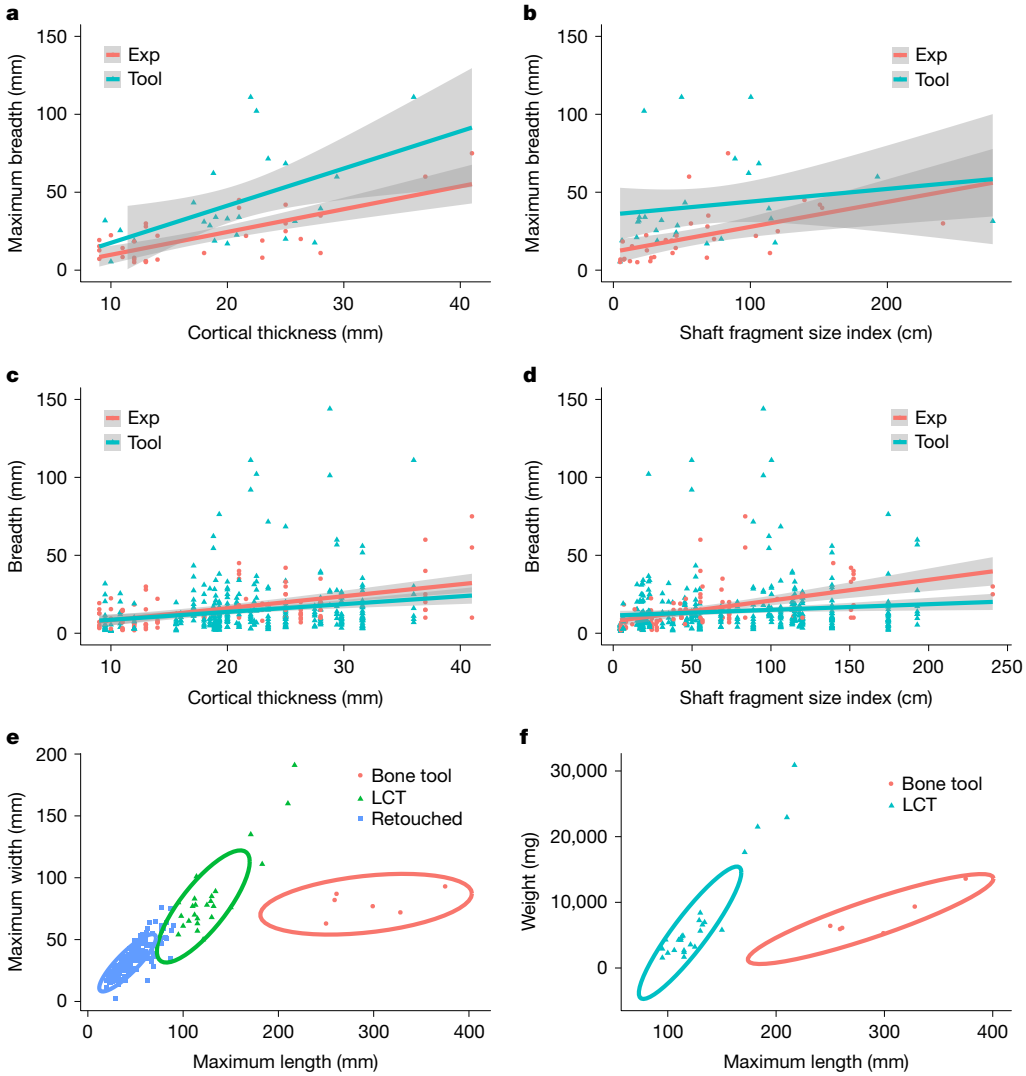

Fig. 2 | Metric comparison of the breadth of flake removal scars relative to the dimension of the bone tools, and the size and weight of the notched bone tools compared with the lithic artefacts found in the same assemblage. **a**–**d**, Scatterplot of the breadth for the most invasive (**a**,**b**) and all (**c**,**d**) removal scars present on the FLK T69 Complex bone tools and on bone fragments produced during experimental (Exp) bone fracturing to expose the marrow of horse[9] and elephant[4] limb bones compared with the cortical thickness (**a**,**c**) and the shaft fragment size index (**b**,**d**). The maximum breadth of the largest flake removal scars on the bone tools and on fragments of limb bones fractured for marrow extraction demonstrates that the former are considerably larger irrespective of the cortical thickness or the shaft fragment size index. The difference in trend observed when considering all flake removal scars is probably due to the production of numerous small contiguous retouch flakes to shape the bone tool edges. **e**,**f**, Length and width (**e**) and length and weight (**f**) comparisons between the T69 Complex bone tools and the lithic assemblage found in the same horizon are shown. Bone tools are more elongated than the LCT, but their current weight falls within the range of variation recorded for the LCT found at the T69 Complex. Trend lines and grey bands indicate the linear regression method and the 90% confidence interval, respectively (**a**–**d**), and the ellipses denote the 90% confidence interval (**e**,**f**).

tools, the T69 Complex knappers invested substantial effort in first producing invasive flake removals to shape the tool and, subsequently, regularizing the resulting edges via trimming. These two steps are documented by comparing the breadth of the flake removal scars with the cortical thickness and the shaft fragment size index (Fig. 2a–d). The most invasive flake removal scars on the bone tools are significantly longer ($F = 21.17$, d.f. = 2 and 461, $P < 0.0001$) than those on fragments of limb bones fractured experimentally for marrow extraction (Fig. 2a,b). The trimming phase, by contrast, produced numerous small contiguous flake removal scars comparable in size—but not in their arrangement—with those on bone fractured experimentally for marrow extraction, which are generally isolated (Fig. 2c,d). Production of blanks for the largest artefacts required striking heavy and sizeable stone percussors against stationary bones[4], whereas morphology of flake removals in all bone tools is compatible with the use of handheld hammerstones during the shaping stage.

Six tools made on more than 2-tonne mammal bones show a recurrent modification pattern to produce a particular shape (Fig. 3 and Extended Data Figs. 7 and 9). With an average of 16.8 removals per specimen, they feature one crescent and one pointed end, coupled with a large invasive notch produced by contiguous removals in the mesial part of the object. Most removal scars making the notch are present on the medullar surface. The pointed end of these tools systematically corresponds to the robust mid-portion of the diaphysis, and the rounded end to the metaphysis. The large notch may have facilitated the prehension of the tool while preserving its sturdy shape and heavy weight.

A function as heavy-duty tools for the larger bone artefacts is suggested by comparison with LCT and smaller retouched lithics from the T69 Complex assemblage. The notched bone tools are larger, more elongated and more intensively shaped than the stone tools—LCT average of 10.1 flake scars per artefact—whereas their current weight falls within the range of recorded variation for LCT found at the site

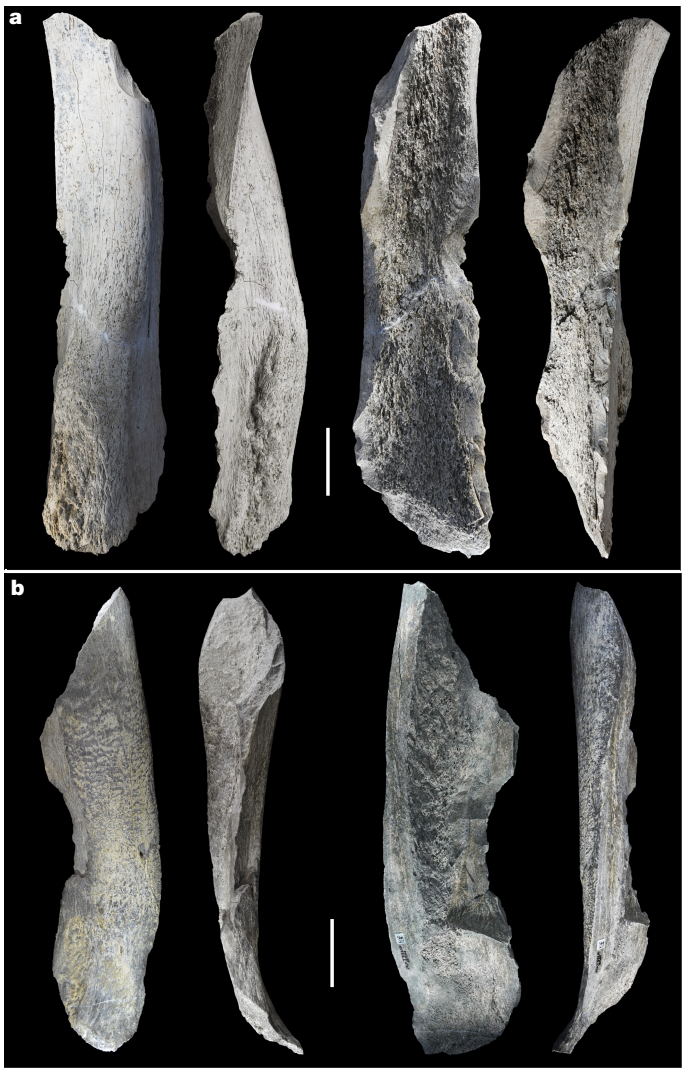

Fig. 3 | Large bone tools made on diaphysis fragments. a, Elephant humerus (accession number T79L10-9047). **b**, Hippopotamus femur (accession number T79L10-18461). Scale bars, 5 cm. See also Extended Data Fig. 7 and Supplementary Videos 6 and 7.

(Fig. 2e,f). Furthermore, distal fracture patterns on some of the specimens evoke their use in percussive and compressive activities[38–41] (Methods; Extended Data Fig. 11).

In summary, to produce bone artefacts at the T69 Complex, hominins selected bones from large mammals and preferentially elephant. Precise anatomical knowledge and understanding of bone morphology and structure are suggested by preference given to thick limb bones as tool blanks. Excellent understanding of bone fracture mechanics is shown by the preferential use of large mammal fresh bones and the application of recurrent flaking procedures. Mental templates are suggested by the production of morphologically similar, elongated, pointed and notched bone tools.

Implications for early bone tool technology

Systematic bone tool production from a single horizon dated to 1.5 Ma at the T69 Complex prompts a reconsideration of the emergence and evolution of bone technology among early hominins. Previous evidence on bone tool production in the Early Stone Age concerned either used unmodified bone fragments[3,11–13], isolated discoveries of possible knapped tools preventing firm conclusions on early hominin behaviours[4,14–17], or bone tools shaped by knapping only occurring after 500 ka[5,6,9,18–21,42]. By contrast, the T69 Complex contains, within the same archaeological assemblage, a set of bone tools that share consistent technological features and signal to the existence of a patterned behaviour.

The T69 Complex bone tools demonstrate that, 1 million years before the production of fully formatted bone bifaces, East African hominins complexified their technology by systematically integrating large, knapped bone tools into it. Such integration occurred at a pivotal time in the evolution of African cultural adaptations—namely, the transition between the late Oldowan and the early Acheulean—and may have had a profound effect on the complexification of behavioural repertoires observed in the latter period[43], including enhancements in cognition and mental templates[44], artefact curation and raw material procurement[45]. This innovation took place at a moment in which large bifacial stone tools had a minor role in their technical systems[46] and had yet to acquire the large size, refined technology and typical symmetrical morphology known for bifaces from subsequent Acheulean assemblages[47]. Particularly at butchery sites of large mammals where suitable raw material was readily available, large heavy bone tools may have fulfilled functions that were later achieved by large bifacial stone tools, which afforded both heavy weight and effective cutting edges. This hypothesis may explain why after the advent of systematic lithic handaxe production, heavy-duty bone tools such as those found at the T69 Complex, potentially less efficient in cutting tasks, may have become rare. In this view, Middle Pleistocene Acheulean bone handaxes[5] could be interpreted as a local transfer to bone of a knapping technology in contexts where scarce availability of optimal lithic raw materials hindered the production of stone LCT.

The alternative scenarios entail that bone technologies appeared and disappeared across more than 1 million years, or were more common in the Early Stone Age than previously thought. In both cases, evidence of such technology is yet to be reported adequately. Preservation bias against organic materials and the limited availability of studies targeting the identification of knapped bone may be masking the widespread and systematic use of osseous technologies, until now thought to appear much later in our evolutionary history. Future research needs to investigate whether similar bone tools were already produced in earlier times, persisted during the Acheulean and eventually evolved into Middle Pleistocene bone bifaces similar in shape, size and technology to their stone counterparts.

Online content

Any methods, additional references, Nature Portfolio reporting summaries, source data, extended data, supplementary information, acknowledgements, peer review information; details of author contributions and competing interests; and statements of data and code availability are available at https://doi.org/10.1038/s41586-025-08652-5.

1. Harmand, S. et al. 3.3-Million-year-old stone tools from Lomekwi 3, West Turkana, Kenya. *Nature* **521**, 310–315 (2015).
2. Proffitt, T. et al. Wild monkeys flake stone tools. *Nature* **539**, 85–88 (2016).
3. Backwell, L. & d'Errico, F. Evidence of termite foraging by Swartkrans early hominids. *Proc. Natl Acad. Sci. USA* **98**, 1358–1363 (2001).
4. Backwell, L. R. & d'Errico, F. The first use of bone tools: a reappraisal of the evidence from Olduvai Gorge, Tanzania. *Palaeontol. Afr.* **40**, 95–158 (2004).
5. Villa, P. et al. Elephant bones for the Middle Pleistocene toolmaker. *PLoS ONE* **16**, e0256090 (2021).
6. Santucci, E. et al. Palaeoloxodon exploitation at the Middle Pleistocene site of La Polledrara di Cecanibbio (Rome, Italy). *Quat. Int.* **406**, 169–182 (2016).
7. Thompson, J. C., Carvalho, S., Marean, C. W. & Alemseged, Z. Origins of the human predatory pattern: the transition to large-animal exploitation by early hominins. *Curr. Anthropol.* **60**, 1–23 (2019).
8. Plummer, T. W. et al. Expanded geographic distribution and dietary strategies of the earliest Oldowan hominins and Paranthropus. *Science* **379**, 561–566 (2023).
9. Doyon, L., Li, Z., Wang, H., Geis, L. & d'Errico, F. A 115,000-year-old expedient bone technology at Lingjing, Henan, China. *PLoS ONE* **16**, e0250156 (2021).
10. Brain, C. K. in *Bone Modification* (eds. Bonnichsen, R. & Sorg, M. H.) 291–297 (Center for the Study of the First Americans, Institute for Quaternary Studies, Univ. Maine, 1989).

11. Backwell, L. R. & d'Errico, F. Additional evidence of early hominid bone tools from South Africa. First attempt at exploring inter-site variability. *Palaeontol. Afr.* **44**, 91–94 (2009).
12. Hanon, R. et al. New evidence of bone tool use by Early Pleistocene hominins from Cooper's D, Bloubank Valley, South Africa. *J. Archaeol. Sci. Rep.* **39**, 103129 (2021).
13. Stammers, R. C., Caruana, M. V. & Herries, A. I. R. The first bone tools from Kromdraai and stone tools from Drimolen, and the place of bone tools in the South African Earlier Stone Age. *Quat. Int.* **495**, 87–101 (2018).
14. Leakey, M. D. *Olduvai Gorge: Excavations in Beds I and II, 1960–1963* Vol. 3 (Cambridge Univ. Press, 1971).
15. Shipman, P. in *Bone Modification* (eds. Bonnichsen, R. & Sorg, M. H.) 317–334 (Center for the Study of the First Americans, Institute for Quaternary Studies, Univ. Maine, 1989).
16. Pante, M., de la Torre, I., d'Errico, F., Njau, J. & Blumenschine, R. Bone tools from Beds II–IV, Olduvai Gorge, Tanzania, and implications for the origins and evolution of bone technology. *J. Hum. Evol.* **148**, 102885 (2020).
17. Sano, K. et al. A 1.4-million-year-old bone handaxe from Konso, Ethiopia, shows advanced tool technology in the early Acheulean. *Proc. Natl Acad. Sci. USA* **117**, 18393–18400 (2020).
18. Rabinovich, R. et al. Elephants at the Middle Pleistocene Acheulian open-air site of Revadim Quarry, Israel. *Quat. Int.* **276–277**, 183–197 (2012).
19. Kretzoi, M. & Dobosi, V. T. *Vértesszőlős: Site, Man and Culture* (Akadémiai Kiadó, 1990).
20. Mania, D. & Vlček, E. *Homo erectus* from Bilzingsleben (GDR) — his culture and his environment. *Anthropologie (Brno)* **25**, 1–45 (1987).
21. Wei, G. et al. First discovery of a bone handaxe in China. *Quat. Int.* **434**, 121–128 (2017).
22. Rosell, J. et al. Bone as a technological raw material at the Gran Dolina site (Sierra de Atapuerca, Burgos, Spain). *J. Hum. Evol.* **61**, 125–131 (2011).
23. Julien, M.-A. et al. Characterizing the Lower Paleolithic bone industry from Schöningen 12 II: a multi-proxy study. *J. Hum. Evol.* **89**, 264–286 (2015).
24. van Kolfschoten, T., Parfitt, S. A., Serangeli, J. & Bello, S. M. Lower Paleolithic bone tools from the 'Spear Horizon' at Schöningen (Germany). *J. Hum. Evol.* **89**, 226–263 (2015).
25. Ma, S. & Doyon, L. Animals for tools: the origin and development of bone technologies in China. *Front. Earth Sci.* **9**, 1138 (2021).
26. d'Errico, F. & Henshilwood, C. S. Additional evidence for bone technology in the southern African Middle Stone Age. *J. Hum. Evol.* **52**, 142–163 (2007).
27. Bouzouggar, A. et al. 90,000 Year-old specialised bone technology in the Aterian Middle Stone Age of North Africa. *PLoS ONE* **13**, e0202021 (2018).
28. Yellen, J. E., Brooks, A. S., Cornelissen, E., Mehlman, M. J. & Stewart, K. A Middle Stone Age worked bone industry from Katanda, Upper Semliki Valley, Zaire. *Science* **268**, 553–556 (1995).
29. d'Errico, F. et al. Technological and functional analysis of 80–60 ka bone wedges from Sibudu (KwaZulu-Natal, South Africa). *Sci. Rep.* **12**, 16270 (2022).
30. Arrighi, S. et al. Bone tools, ornaments and other unusual objects during the Middle to Upper Palaeolithic transition in Italy. *Quat. Int.* **551**, 169–187 (2020).
31. d'Errico, F., Borgia, V. & Ronchitelli, A. Uluzzian bone technology and its implications for the origin of behavioural modernity. *Quat. Int.* **259**, 59–71 (2012).
32. Langley, M. C. et al. Bows and arrows and complex symbolic displays 48,000 years ago in the South Asian tropics. *Sci. Adv.* **6**, eaba3831 (2020).
33. Zhang, S. et al. Ma'anshan cave and the origin of bone tool technology in China. *J. Archaeolog. Sci.* **65**, 57–69 (2016).
34. d'Errico, F. et al. The origin and evolution of sewing technologies in Eurasia and North America. *J. Hum. Evol.* **125**, 71–86 (2018).
35. Fujioka, T. et al. Direct cosmogenic nuclide isochron burial dating of early Acheulian stone tools at the T69 Complex (FLK West, Olduvai Bed II, Tanzania). *J. Hum. Evol.* **165**, 103155 (2022).
36. Villa, P. & Bartram, L. Flaked bone from a hyena den. *Paléo* **8**, 143–159 (1996).
37. Villa, P. et al. The archaeology and paleoenvironment of an Upper Pleistocene hyena den: an integrated approach. *J. Archaeolog. Sci.* **37**, 919–935 (2010).
38. Burke, A. & d'Errico, F. A Middle Palaeolithic bone tool from Crimea (Ukraine). *Antiquity* **82**, 843–852 (2008).
39. Tartar, É. The recognition of a new type of bone tools in Early Aurignacian assemblages: implications for understanding the appearance of osseous technology in Europe. *J. Archaeol. Sci.* **39**, 2348–2360 (2012).
40. Kozlikin, M. B., Rendu, W., Plisson, H., Baumann, M. & Shunkov, M. V. Unshaped bone tools from Denisova Cave, Altai. *Archaeol. Ethnol. Anthropol. Eurasia* **48**, 16–28 (2020).
41. Fisher, D. C. Taphonomic analysis of late Pleistocene mastodon occurrences: evidence of butchery by North American Paleo-Indians. *Paleobiology* **10**, 338–357 (1984).
42. Anzidei, A. P. et al. Ongoing research at the late Middle Pleistocene site of La Polledrara di Cecanibbio (central Italy), with emphasis on human–elephant relationships. *Quat. Int.* **255**, 171–187 (2012).
43. de la Torre, I. The origins of the Acheulean: past and present perspectives on a major transition in human evolution. *Phil. Trans. R. Soc. B* **371**, 20150245 (2016).
44. Suwa, G., Asfaw, B., Sano, K. & Beyene, Y. Reply to Barkai: implications of the Konso bone handaxe. *Proc. Natl Acad. Sci. USA* **117**, 30894–30895 (2020).
45. Presnyakova, D. et al. Site fragmentation, hominin mobility and LCT variability reflected in the early Acheulean record of the Okote Member, at Koobi Fora, Kenya. *J. Hum. Evol.* **125**, 159–180 (2018).
46. de la Torre, I. & Mora, R. The Transition to the Acheulean in East Africa: an assessment of paradigms and evidence from Olduvai Gorge (Tanzania). *J. Archaeol. Method Theory* **21**, 781–823 (2014).
47. Beyene, Y. et al. The characteristics and chronology of the earliest Acheulean at Konso, Ethiopia. *Proc. Natl Acad. Sci. USA* **110**, 1584–1591 (2013).

Methods

Site context

Location and age. The T69 Complex (WGS84 UTM Zone 36S, x = 760990; y = 9669250) is located in the Frida Leakey Korongo (FLK) West outcrop, within the Main Gorge at Olduvai Gorge, in northern Tanzania. Excavations were conducted annually through eight field seasons between 2015 and 2022. Seven trenches (T69, T71, T74, T75, T77, T78 and T79) were dug at the site, of which three (T71, T74 and T75) yielded no archaeological materials (T71 was placed above and T74–T75 below the fossil-bearing horizons). Separate names were given to the trenches as test pits progressed around the main outcrop, but eventually they were all linked up into one single excavation area (Supplementary Video 1) named T69 Complex, after the first trench we dug at the FLK West locality.

Stratigraphically, the site is positioned in Olduvai Bed II, which overlays Bed I and is capped by Bed III (Extended Data Fig. 1e). The top of Bed I (Tuff IF) is dated to 1.803 ± 0.002 Ma[48], whereas the base of Bed III is estimated at 1.14 ± 0.05 Ma[49]. Within Bed II, the T69 Complex is placed within a sandstone bed in the Tuff IIC stratigraphic interval[50] that marks the transition between Middle and Upper Bed II[14], and sits 7 m above the Bird Print Tuff and 4 m below Tuff IID[35]. A tuff located 20 cm below the Bird Print Tuff[51] has been dated at 1.664 ± 0.019 Ma[52], and an average age of 1.339 ± 0.024 Ma has been estimated for Tuff IID[53]. The bone tool level in the T69 Complex has been dated at 1.48 ± 0.2 (1σ) Ma using direct cosmogenic nuclide isochron burial dating[35], which is consistent with the constraining ages available for Beds I, II and III (Extended Data Fig. 1e).

During the Tuff IIC interval, the Olduvai perennial palaeolake was constrained by the graben between the Fifth and FLK faults. The FLK locality was positioned in the southeastern lake-margin zone, with drainage inputs towards the north-northeast[50]. The T69 Complex deposits are dominated by the fluvial and lacustrine processes occurring at the eastern margin of the Bed II palaeolake[50]. The lower interval consists of alluvial massive sands and silty decantation facies (Extended Data Fig. 1d). These deposits were partially eroded by water flows, which led to the sedimentation of the sandstone bed containing the bone tool horizon. This sandstone has a sheet-like geometry and contains mainly tuffaceous facies with a massive or poorly bedded structure. The sandstone bed includes local lenses of augitic cross-laminated facies more abundant towards the base, and discontinuous patches of cemented very fine sandstone towards the top. Thin sections of the sandstone indicate a clay matrix and subrounded to rounded grains, from very coarse to fine in size, that locally include claystone rip-up subrounded clasts (Extended Data Fig. 1f). These sedimentological features suggest that cross-laminated facies were generated by local phases of traction and sedimentation under low regime flow conditions, whereas predominant massive or weakly bedded facies were formed by relatively rapid deposition of suspended load during decreasing flood. The sandy facies were buried by progradation of lacustrine brown clays (Extended Data Fig. 1d).

Excavation and sample preparation. Sedimentary units with no archaeological remains overburdening fossiliferous beds, which in some parts of the outcrop were more than 6 m thick, were removed manually with larger picks. Excavation of archaeological units initiated with small picks, and when remains were found, these were uncovered sequentially with screwdrivers, dental tools and wooden sticks. Each item found in situ, regardless of its size, was given a unique ID, positioned three-dimensionally with a total station, and recorded following the protocols outlined by de la Torre et al.[54]. Azimuth (dip direction, 0–360°) and dip angle (0–90°) of the major axis of suitable elongated items[55] were recorded with compass and clinometer during the excavation process. All sediment collected from the archaeological units was dry-screened with 2-mm-mesh sieves. All items with an individual ID were hand-labelled, and a QR code was attached and added to a geographical information system that integrates all archaeological information for the FLK site.

Following conservation protocols detailed elsewhere[56], some bone tools were stabilized by temporary consolidation with cyclododecane (a cyclic alkane hydrocarbon) before being lifted from the excavation. Solutions of paraloid B-72 (ethyl methacrylate–methyl acrylate co-polymer) or B-44 (methylmethacrylate–ethylacrylate) on acetone were also used. Mechanical removal of sedimentary accretions avoided contact with bone surfaces. When necessary, excessive consolidant was removed, breaks aligned and further consolidation carried out. Gaps or cracks that undermined structural condition of fossils were filled with B-44 or B-72 mixed with acetone and microscopic glass spheres.

Site formation. The T69 Complex bone horizon spans an average thickness of approximately 50 cm and was excavated across a surface of 295 m^2 (Extended Data Fig. 2 and Supplementary Video 2). Using ArcGIS Pro (v3.3), the horizontal distribution pattern was tested through an average nearest neighbour analysis that compared the actual distance between items to a hypothetical random sample[57]. The complete assemblage and the lithic and fossil assemblages showed a significantly clustered distribution (P = 0.000; Extended Data Fig. 3-1), whereas the bone tools were randomly distributed across the clusters (P = 0.6785).

Orientation[58,59] and fabric analyses[55,60] were conducted using Oriana software (v3.13) to investigate potential rearrangements of the assemblage. Orientation angular histograms show a circular-shaped distribution (Extended Data Fig. 3-2a), which becomes more homogeneous when axial values are projected (Extended Data Fig. 3-2b). When considering orientation as axial data (0–180°), statistical tests do not allow rejecting the null hypothesis of uniformity. By contrast, all azimuthal data statistical tests reject the uniform distribution against unimodal and plurimodal distributions, indicating a preferential orientation pattern with a mean vector at N22° E (see statistical results in table 1 in Supplementary Data 1). Stereographic projection of azimuth and dip values showed that most of the data concentrated around the external area and dominated by low dip angles (Extended Data Fig. 3-2c). Fabrics indicate a gridle or planar shape (Extended Data Fig. 3-2d,e), with eigenvector 1 pointing towards N27° E and thus coinciding with the mean vector direction (table 2 in Supplementary Data 1).

In summary, horizontal distribution patterns do not indicate a differential distribution between fossils and lithics, with both groups appearing together in clusters and bone tools scattered randomly across the excavation surface. The planar or girdle fabric with low dip angles suggests that archaeological items were accumulated on a subhorizontal surface and did not experience post-depositional vertical dispersion. Nonetheless, azimuthal data in the horizontal dimension indicate a notable influence of the dip direction, characterized by a mean vector that coincides with the north-northeast palaeo-drainage trend estimated by Hay[50] in the lake-margin zone near the FLK locality. This suggests that the archaeological assemblage may have experienced some rearrangements by the alluvial flows depositing the sandstone bed. Given the generally excellent preservation of the archaeological items, the sheer abundance of less than 2 cm lithics, the sedimentological features of the sandstone bed (see the 'Location and age' section), and the orientated but scarcely clustered angular pattern, this gentle reorganization would be produced by low-energy flood-sheets with a poor sorting capacity, in which the item direction was determined by the depositional surface.

Faunal assemblage. The T69 Complex fossil assemblage (n = 22,832; bones of 2 cm or more = 45.3%; bones of less than 2 cm = 54.7%) contains abundant mammal (more than 11,627), reptile (n = 1,453), fish (n = 1,084) and bird (n = 286) specimens. Mammal bones of 2 cm or more (n = 8,930) were sampled for full zooarchaeological analysis following refs. 56,61,62. This zooarchaeological control sample (ZCS; n = 2,075) included (1) all items identified as bone tools, (2) all proboscidean fossils (given their relevance among the bone tool assemblage, the entire T69 Complex fossil collection was inspected to ensure all elephant specimens were analysed), and (3) a randomly selected sample from all other

2 cm or more mammal bone specimens. Whenever possible, the taxa and skeletal element were recorded. Otherwise, the specimens were attributed to a mammal size class based on their cortical thickness following Bunn[63]. Fresh and weathered bone fractures were distinguished based on criteria available in the literature[64–71].

The ZCS skeletal part profile is dominated by axial bones (ribs and vertebrae), followed by appendicular elements (particularly tibia, femur, humerus and unidentifiable long bone fragments; tables 3 and 4 in Supplementary Data 1). Taxonomically, the ZCS assemblage is dominated by Bovidae (n = 691; 33.3%) and Hippopotamidae (n = 233; 11.2%), with considerably lower proportions of Equidae (n = 49; 2.3%) and Elephantidae (n = 22; 1.1%), and residual presence of other taxa such as Rhinocerotidae (n = 8; 0.4%), Suidae (n = 7; 0.3%) and others (n = 2; less than 0.1%; table 5 in Supplementary Data 1). The assemblage contains at least 16 different individuals from 10 distinct species (table 6 in Supplementary Data 1): *Hippopotamus* cf. *gorgops* (minimum number of individuals (MNI) = 4), *Equus* sp. (MNI = 2), *Elephas* cf. *recki* (MNI = 2), *Diceros* cf. *bicornis* (MNI = 2), *Damaliscus* cf. *lunatus* (MNI = 1), *Connochaetes* aff. *gentryi* (MNI = 1), *Eudorcas* cf. *thomsonii* (MNI = 1), *Hippotragus gigas* (MNI = 1), *Kobus* sp. (MNI = 1) and *Tragelaphus* aff. *imberbis* (MNI = 1). Overall, taxonomic composition and animal size distribution (table 7 in Supplementary Data 1) of the T69 Complex site suggests similar ecological conditions to the modern-day Serengeti ecosystem, with open and seasonal grassland habitats dominated by large communities of size 2 and 3 bovids near rivers and at the margin of an alkaline lake that accommodated hippopotamids, fish and crocodilians[72,73].

Cut marks (present in more than 5.5% of the ZCS specimens) and percussion marks (more than 3.1%) indicate that early humans butchered carcasses at the site (tables 8 and 9 in Supplementary Data 1). According to the tooth-marked bone proportion (more than 2.4%), carnivores had a lesser role in the formation of the assemblage (table 10 in Supplementary Data 1). A short period of subaerial exposure is documented in 39.8% of specimens, although stage 2 (ref. 74) bones dominate the sample and more weathered bones are also present (table 11 in Supplementary Data 1). All these taphonomic signatures indicate separate assemblage formation episodes and are consistent with the alluvial dynamics that characterize the T69 Complex depositional environment.

Site function. Taxa represented, skeletal part profiles and taphonomic patterns indicate that hominins occupied a floodplain environment where they accessed relatively complete carcasses of hippopotamus. Other mammal body parts that show anthropogenic modifications—including bovids (cut-marked bones) and elephants (flaked bones)—were potentially transported by hominins to the site. Hominins also imported large quantities of quartzite from the nearby hill of Naibor Soit[50] to produce stone tools. The input of other biotic as well as abiotic agents to the formation of the assemblage is attested by the presence of tooth-marked bones—indicating carnivore action—birds, reptiles and fish—unrelated to the formation of the anthropogenic assemblage—and the sedimentary evidence—pointing at gentle rearrangements of parts of the deposit.

The large size of both the stone tool and bone assemblages suggests that hominins visited the area repeatedly, probably attracted by the availability of dead hippopotamus. Exploitation of hippopotamus carcasses was not limited to meat procurement, but also to the production of bone tools. Cut marks produced by lithics clearly indicate that stone tools imported from Naibor Soit had a role in the butchery activities, but we argue that hominins were also importing bone raw materials; elephant fossils are rare in the T69 Complex faunal composition, whereas they are overrepresented in the bone tool assemblage. We hypothesize that bone-tool makers accessed elephant limbs elsewhere and shaped large diaphyseal fragments that were then imported to the T69 Complex and used in percussive and compressive activities, potentially related to butchery of the hippopotamus carcasses that attracted hominins to the area.

Bone tools

Taphonomy. Bone tools (n = 27) with most conspicuous technological features were recognized onsite during the excavation process (Supplementary Video 2), whereas others were identified during the inspection of the entire sample of mammal bones of 2 cm or longer. Each specimen was first examined with a magnifying glass with incident light. Anthropogenic modifications were distinguished from natural modifications based on published criteria[41,74–85], with a particular attention on the natural and anthropogenic processes that could produce flaking scars on faunal remains, such as trampling[86–88], carnivore alterations[36,37,83,89,90] and marrow extraction[4,9,91–95] (see below and Supplementary Data 3).

Bone tool analysis and comparison with archaeological and experimental samples. The archaeological material considered in the present study comprised: (1) the 27 bone specimens bearing features, that is, flake scars, impact and morphology, that led us to consider them as bone tools (henceforth, BTS; Figs. 1 and 3 and Extended Data Figs. 6–10). (2) A sample of 4,507 long bone fragments from the same excavation (henceforth, random control sample (RCS)). The RCS was selected to verify whether the bone tools stood out morphologically when compared with the rest of the fauna or instead represented an extreme in size variation, that is, in maximum length, width and thickness of the bone fragments. (3) A subsample of 250 long bone fragments from RCS (henceforth, random control subsample (RCSS)). The RCSS was selected to verify whether the number of flake removal scars observed on the BTS stood out from other specimens in the faunal assemblage or instead represented an extreme in variation.

To establish whether marrow extraction activities could have produced a flaking pattern akin to that observed on the RCSS and BTS, we compared the T69 Complex specimens with two published experimental samples of large mammal long bones fractured to expose marrow. The first, henceforth, experimental sample 1 (ES1), consisted of nine elephant long bones fractured by knapping that produced 107 diaphyseal fragments[4]. The second, ES2, derives from the fracturing of six horse long bones by knapping, which resulted in 33 diaphyseal fragments and 284 flakes and splinters[9]. The maximum length, width, thickness and cortical thickness of the specimens included in BTS, ES1 and ES2 were collected using a digital calliper. The following variables were recorded for specimens with flake removal scars: number of scars, the location of each scar (cortical or medullar surface, distal, proximal, right or left lateral edge), their arrangement (isolated, contiguous or series of contiguous flakes) and the breadth of each scar. The contiguous category includes both adjacent and overlapping flake removal scars. Series of contiguous flake scars imply two or more groups of contiguous scars separated by an unmodified edge. The breadth of the flake removal scars was compared with the cortical thickness of the diaphyseal fragment and with the shaft fragment size index, that is, the product of the maximum length and width (in centimetres) divided by two[4], to detect anomalously invasive flake removal scars on BTS compared with those recorded for the ES1 and ES2 specimens.

Recurrent patterns in the anthropogenic modification of bone fragments were sought in the frequency, size and arrangement of flake removal scars as well as on fractures resulting from potential use. Technological features were described following conventions proposed by Inizan et al.[96] and adapted to bone tools analysis by Pante et al.[16]. Size comparison was done between the heavy-duty bone tools, that is, a subsample of the BTS, and the lithic LCT and retouched flakes found in the T69 Complex assemblage. Finally, the weight of the heavy-duty bone tools and lithic LCT was also compared.

All bone tools were photographed with a Nikon D7500 camera (Nikon DX 18–140 mm 1:3.5–5.6 and Nikon N 105 mm 1:2.8 lenses), and 3D scanned with an Artec Space Spider 3D scanner. Relevant bone surface modifications were analysed with a Leica DVM6 digital microscope

(Planapo FOV 12.55 and 43.75 objectives, up to ×675). The quantitative analyses and graphs were done in R-CRAN (v4.4.1)[97].

Reporting summary

Further information on research design is available in the Nature Portfolio Reporting Summary linked to this article.

Data availability

All data generated or analysed during this study are included in this published article and its Supplementary Information files.

48. Deino, A. L. 40Ar/39Ar dating of Bed I, Olduvai Gorge, Tanzania, and the chronology of early Pleistocene climate change. *J. Hum. Evol.* **63**, 251–273 (2012).
49. Deino, A. L. et al. Chronostratigraphy and age modeling of Pleistocene drill cores from the Olduvai Basin, Tanzania (Olduvai Gorge Coring Project). *Palaeogeogr. Palaeoclimatol. Palaeoecol.* **571**, 109990 (2021).
50. Hay, R. L. *Geology of the Olduvai Gorge* (Univ. California Press, 1976).
51. Uribelarrea, D. et al. A reconstruction of the paleolandscape during the earliest Acheulian of FLK West: the co-existence of Oldowan and Acheulian industries during lowermost Bed II (Olduvai Gorge, Tanzania). *Palaeogeogr. Palaeoclimatol. Palaeoecol.* **488**, 50–58 (2017).
52. Diez-Martín, F. et al. The origin of the Acheulean: the 1.7 million-year-old site of FLK West, Olduvai Gorge (Tanzania). *Sci. Rep.* **5**, 17839 (2015).
53. Domínguez-Rodrigo, M. et al. First partial skeleton of a 1.34-million-year-old *Paranthropus boisei* from Bed II, Olduvai Gorge, Tanzania. *PLoS ONE* **8**, e80347 (2013).
54. de la Torre, I., Arroyo, A., Proffitt, T., Martín Ramos, C. & Theodoropoulou, A. Archaeological fieldwork techniques in Stone Age sites: some case studies. *Treballs d'Arqueol.* **20**, 21–40 (2014).
55. Benito-Calvo, A., Martínez-Moreno, J., Jordá Pardo, J. F., de la Torre, I. & Mora Torcal, R. Sedimentological and archaeological fabrics in Palaeolithic levels of the south-eastern Pyrenees: Cova Gran and Roca dels Bous sites (Lleida, Spain). *J. Archael. Sci.* **36**, 2566–2577 (2009).
56. Pante, M. C. et al. The carnivorous feeding behavior of early Homo at HWK EE, Bed II, Olduvai Gorge, Tanzania. *J. Hum. Evol.* **120**, 215–235 (2018).
57. Ebdon, D. *Statistics in Geography* 2nd edn (Blackwell, 1985).
58. Fisher, N. I. *Statistical Analysis of Circular Data* (Cambridge Univ. Press, 1995).
59. de la Torre, I. & Benito-Calvo, A. Application of GIS methods to retrieve orientation patterns from imagery: a case study from Beds I and II, Olduvai Gorge (Tanzania). *J. Archael. Sci.* **40**, 2446–2457 (2013).
60. Bertran, P., Hétu, B., Texier, J.-P. & van Steijn, H. Fabric characteristics of subaerial slope deposits. *Sedimentology* **44**, 1–16 (1997).
61. Binford, L. R. *Nunamiut Ethnoarchaeology: a Case Study in Archaeological Formation Processes* (Academic Press, 1978).
62. Marean, C. W. & Kim, S. Y. Mousterian large-mammals from Kobeh Cave. *Curr. Anthropol.* **39**, 79–113 (1998).
63. Bunn, H. T. *Meat-eating and Human Evolution: Studies on the Diet and Subsistence Patterns of Plio-Pleistocene Hominids in East Africa* (Univ. California, Berkeley, 1982).
64. Coe, M. The decomposition of elephant carcasses in the Tsavo (East) National Park, Kenya. *J. Arid. Environ.* **1**, 71–86 (1978).
65. Haynes, G. Frequencies of spiral and green-bone fractures on ungulate limb bones in modern surface assemblages. *Am. Antiq.* **48**, 102–114 (1983).
66. Haynes, G. Longitudinal studies of African elephant death and bone deposits. *J. Archaeol. Sci.* **15**, 131–157 (1988).
67. Karr, L. P. & Outram, A. K. Bone degradation and environment: understanding, assessing and conducting archaeological experiments using modern animal bones. *Int. J. Osteoarchaeol.* **25**, 201–212 (2015).
68. Pokines, J. T. et al. The effects of repeated wet–dry cycles as a component of bone weathering. *J. Archaeol. Sci. Rep.* **17**, 433–441 (2018).
69. Haynes, G., Krasinski, K. & Wojtal, P. Elephant bone breakage and surface marks made by trampling elephants: implications for interpretations of marked and broken *Mammuthus* spp. bones. *J. Archaeol. Sci. Rep.* **33**, 102491 (2020).
70. Haynes, G., Krasinski, K. & Wojtal, P. A study of fractured Proboscidean bones in recent and fossil assemblages. *J. Archaeol. Method Theory* **28**, 956–1025 (2021).
71. Haynes, G. & Wojtal, P. Weathering stages of Proboscidean bones: relevance for zooarchaeological analysis. *J. Archaeol. Method Theory* **30**, 495–535 (2023).
72. Bibi, F. et al. Paleoecology of the Serengeti during the Oldowan–Acheulean transition at Olduvai Gorge, Tanzania: the mammal and fish evidence. *J. Hum. Evol.* **120**, 48–75 (2018).
73. Uno, K. T. et al. Large mammal diets and paleoecology across the Oldowan–Acheulean transition at Olduvai Gorge, Tanzania from stable isotope and tooth wear analyses. *J. Hum. Evol.* **120**, 76–91 (2018).
74. Behrensmeyer, A. K. Taphonomic and ecologic information from bone weathering. *Paleobiology* **4**, 150–162 (1978).
75. Haynes, G. A guide for differentiating mammalian carnivore taxa responsible for gnaw damage to herbivore limb bones. *Paleobiology* **9**, 164–172 (1983).
76. Haynes, G. *Mammoths, Mastodonts, and Elephants: Biology, Behavior and the Fossil Record* (Cambridge Univ. Press, 1991).
77. Shipman, P., Fisher, D. C. & Rose, J. J. Mastodon butchery: microscopic evidence of carcass processing and bone tool use. *Paleobiology* **10**, 358–365 (1984).
78. Noe-Nygaard, N. Taphonomy in archaeology with special emphasis on man as a biasing factor. *J. Danish Archaeol.* **6**, 7–62 (1987).
79. Noe-Nygaard, N. Man-made trace fossils on bones. *Hum. Evol.* **4**, 461–491 (1989).
80. Lyman, R. L. *Vertebrate Taphonomy* (Cambridge Univ. Press, 1994).
81. Fisher, J. W. Jr Bone surface modifications in zooarchaeology. *J. Archaeol. Method Theory* **2**, 7–68 (1995).
82. Hutson, J. M., Burke, C. C. & Haynes, G. Osteophagia and bone modifications by giraffe and other large ungulates. *J. Archaeolog. Sci.* **40**, 4139–4149 (2013).
83. Fernández-Jalvo, Y. & Andrews, P. *Atlas of Taphonomic Identifications* (Springer Dordrecht, 2016).
84. Wadley, L. A camera trap record of scavengers at a kudu carcass: implications for archaeological bone accumulations. *Trans. R. Soc. South Africa* **75**, 245–257 (2020).
85. Backwell, L., Huchet, J.-B., du Guesclin Harrison, J. & d'Errico, F. in *Manual of Forensic Taphonomy* (eds. Pokines, J. T. & Symes, S. A.) 631–666 (CRC Press, 2021).
86. Behrensmeyer, A. K., Gordon, K. D. & Yanagi, G. T. Trampling as a cause of bone surface damage and pseudo-cutmarks. *Nature* **319**, 768–771 (1986).
87. Olsen, S. L. & Shipman, P. Surface modification on bone: trampling versus butchery. *J. Archaeol. Sci.* **15**, 535–553 (1988).
88. Blasco, R., Rosell, J., Fernández Peris, J., Cáceres, I. & Vergès, J. M. A new element of trampling: an experimental application on the level XII faunal record of Bolomor Cave (Valencia, Spain). *J. Archaeol. Sci.* **35**, 1605–1618 (2008).
89. Cruz-Uribe, K. Distinguishing hyena from hominid bone accumulations. *J. Field Archaeol.* **18**, 467–486 (1991).
90. Brugal, J.-P. & Fourvel, J.-B. Puncture game: let's play with the canines of carnivores. *Quat. Sci. Adv.* **13**, 100129 (2024).
91. Vincent, A. *L'outillage Osseux au Paléolithique Moyen: une Nouvelle Approche* (Université de Paris X, 1993).
92. Madrigal, T. C. & Blumenschine, R. J. Preferential processing of high return rate marrow bones by Oldowan hominids: a comment on Lupo. *J. Archaeol. Sci.* **27**, 739–741 (2000).
93. Outram, A. K. A new approach to identifying bone marrow and grease exploitation: why the "indeterminate" fragments should not be ignored. *J. Archaeol. Sci.* **28**, 401–410 (2001).
94. Blasco, R., Domínguez-Rodrigo, M., Arilla, M., Camarós, E. & Rosell, J. Breaking bones to obtain marrow: a comparative study between percussion by batting bone on an anvil and hammerstone percussion. *Archaeometry* **56**, 1085–1104 (2014).
95. Vettese, D. et al. Towards an understanding of hominin marrow extraction strategies: a proposal for a percussion mark terminology. *Archaeol. Anthropol. Sci.* **12**, 48 (2020).
96. Inizan, M.-L., Reduron, M., Roche, H. & Tixier, J. *Préhistoire de La Pierre Taillée: Technologie de La Pierre Taillée, Suivi Par Un Dictionnaire Multilingue Allemand, Anglais, Arabe, Espagnol, Français, Grec, Italien, Portugais* Vol. 4 (C.R.E.P., 1995).
97. R Core Team. *R: A Language and Environment for Statistical Computing* http://www.R-project.org (R Foundation for Statistical Computing, 2021).
98. Jorayev, G., Wehr, K., Benito-Calvo, A., Njau, J. & de la Torre, I. Imaging and photogrammetry models of Olduvai Gorge (Tanzania) by unmanned aerial vehicles: a high-resolution digital database for research and conservation of Early Stone Age sites. *J. Archaeol. Sci.* **75**, 40–56 (2016).
99. Vollmer, F. W. A triangular fabric plot with applications for structural analysis. *Am. Geophys. Union Trans.* **70**, 463 (1989).
100. Benn, D. Fabric shape and the interpretation of sedimentary fabric data. *J. Sediment. Res.* **64**, 910–915 (1994).
101. de la Torre, I. & Mora, R. Technological behaviour in the early Acheulean of EF-HR (Olduvai Gorge, Tanzania). *J. Hum. Evol.* **120**, 329–377 (2018).

Acknowledgements Permits issued to the Olduvai Gorge Archaeology Project to conduct research at Olduvai were granted by the Tanzanian Commission of Science and Technology, Department of Antiquities (Ministry of Natural Resources and Tourism) and Ngorongoro Conservation Area Authority. We thank the Olduvai fieldwork crew who participated in the 2015–2022 excavations at the T69 Complex, particularly to A. Lucas and A. Venance; the CSIC-Pleistocene Archaeology Laboratory personnel (particularly A. Seisdedos and C. Fernández) for their assistance in producing the supplementary videos, the spatial analysis and Extended Data Fig. 2; and C. Sáiz and B. Notario (CENIEH) for thin-section preparation and photography. L.D. and F.d'E. were financially supported by the following agencies: Initiative d'Excellence IdEx, University of Bordeaux, Talent program grant no. 191022-001 (to F.d'E. and L.D.); French government in the framework of the University of Bordeaux's IdEx 'Investments for the Future' program/GPR 'Human Past' (to F.d'E. and L.D.); the Research Council of Norway, Centres of Excellence (SFF), Centre for Early Sapiens Behaviour, SapienCE grant no. 262618 (to F.d'E.); European Research Council (Synergy grant for the project Evolution of Cognitive Tools for Quantification (QUANTA), no. 951388; to F.d'E.) and (Starting grant for the project Pleistocene Expedient Osseous Technology (ExOsTech), no. 101161065; to L.D.)). Fieldwork grants by Fundación Palarq and the Spanish Ministry of Culture, and major funding by the European Research Council-Advanced grants: Biogeographic and Cultural Adaptations of Early Humans during the First Intercontinental Dispersals (BICAEHFID, no. 832980), are gratefully acknowledged.

Author contributions I.d.l.T. and J.K.N. directed the Olduvai Gorge Archaeology Project fieldwork. I.d.l.T. and R.M. supervised excavations. A.B.-C. conducted the geological study. R.F.P. supervised conservation of the faunal assemblage. I.M. conducted the zooarchaeological analysis. I.d.l.T., J.K.N., F.d'E. and L.D. analysed the bone tools. Quantitative analysis was produced by L.D. (bone tools), A.B.-C. (orientation and fabrics) and I.M. (zooarchaeology). A.T. produced the imagery and collected the 3D scan data. I.d.l.T., F.d'E. and L.D. wrote the first draft. All authors discussed the results and contributed to the manuscript.

Competing interests The authors declare no competing interests.

Additional information

Supplementary information The online version contains supplementary material available at https://doi.org/10.1038/s41586-025-08652-5.

Correspondence and requests for materials should be addressed to Ignacio de la Torre or Jackson K. Njau.

Peer review information *Nature* thanks Marta Mirazon Lahr, Jessica Thompson and the other, anonymous, reviewer(s) for their contribution to the peer review of this work.

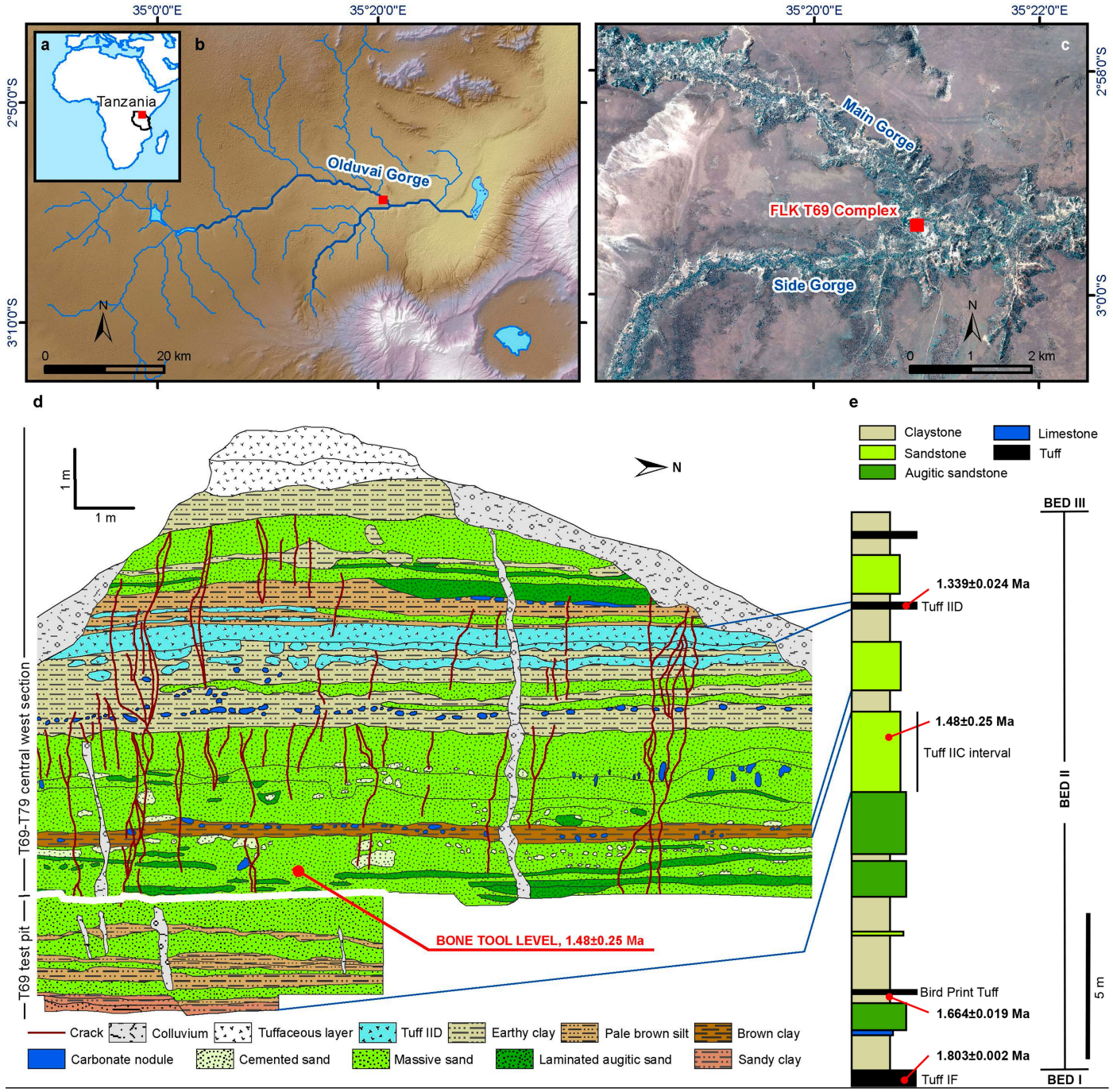

Extended Data Fig. 1 | See next page for caption.

Extended Data Fig. 1 | Geographic and stratigraphic context of the FLK T69 Complex site. a, Location of Olduvai Gorge in Tanzania. **b**, Main geographical features of the Olduvai Basin. The geographical image was adapted from NASA (https://lpdaac.usgs.gov/products/astgtmv003/), USGS. **c**, Position of the T69 Complex in the Main Gorge at Olduvai. The geographical image was adapted with permission from ref. 98, Elsevier. **d**, Stratigraphic position of the bone tool level shown on a composite section of the deepest part of trench T69 and the central area of the T69-T79 west section. **e**, Position of the T69 Complex within the general chrono-stratigraphic sequence of Bed II in the FLK area. Dates by[35,48,52,53]. **f**, Normal (left) and polarized (right) thin section photographs of the sandstone containing the bone tool horizon.

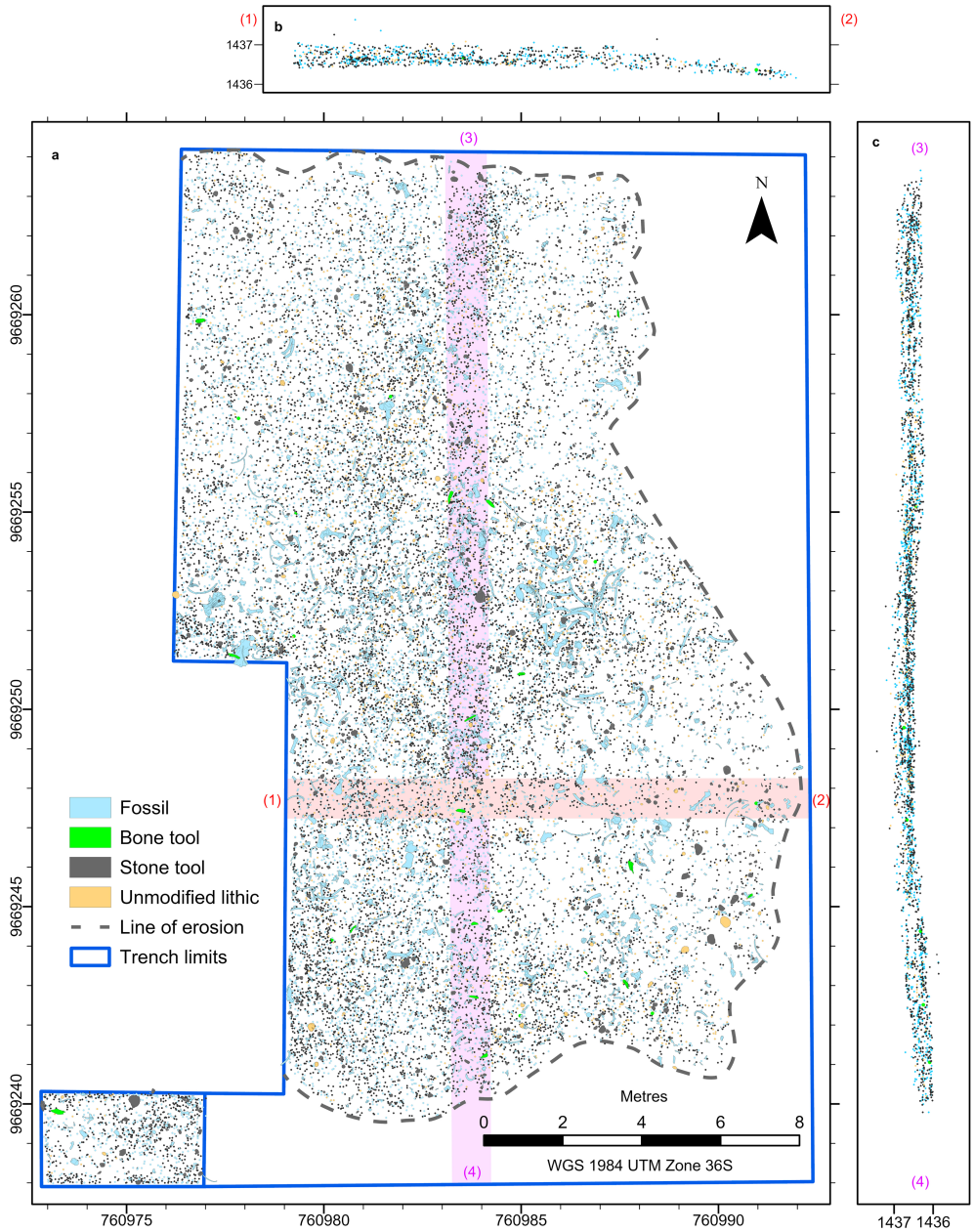

Extended Data Fig. 2 | Distribution map of the T69 Complex bone tool horizon. a, Plan view. **b**, East-West cross section within a 1-metre-wide area between (1) and (2). **c**, North-South cross section within a 1-metre-wide area between (3) and (4). See also Supplementary Video 2.

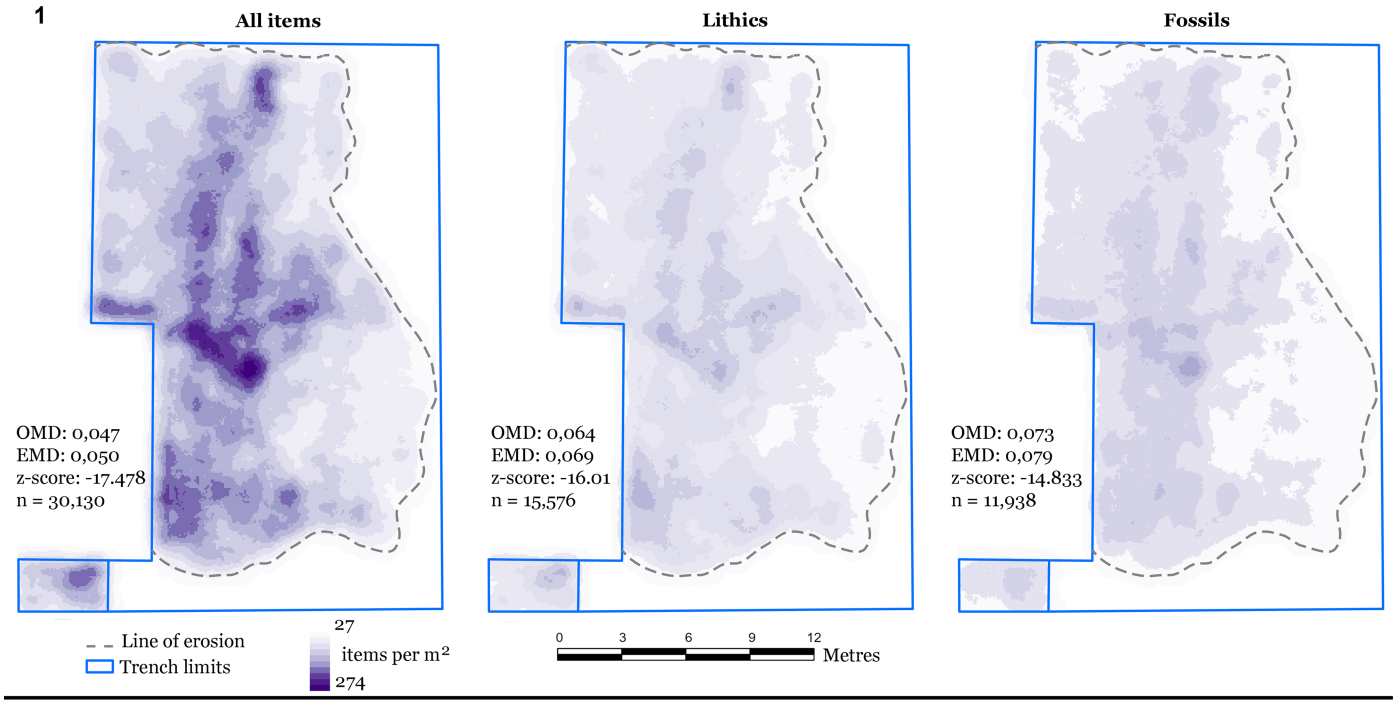

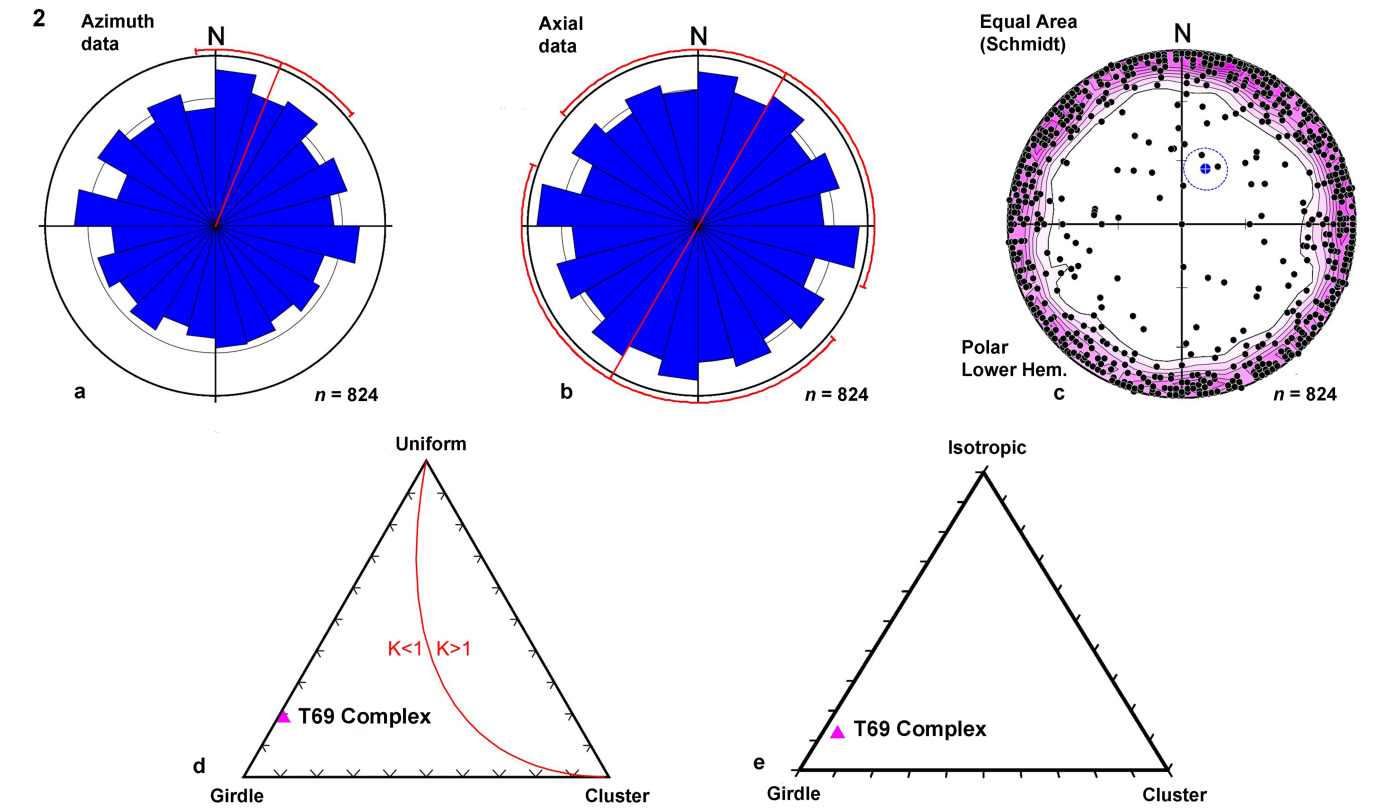

Extended Data Fig. 3 | Horizontal distribution density maps (1) and angular histograms and stereographic projections (2) of lithics and fossils from the T69 Complex bone tool horizon. 1) Observed Mean Distance (OMD) and Expected Mean Distance (EMD) are expressed in metres. *P*-values of complete, lithic and bone assemblages = 0.000. *P*-value of bone tool distribution = 0.6785. **2)** Orientation of items with elongation index >1.6[60] calculated as azimuthal (**a**) and axial data (**b**). **c**, Stereographic projection of azimuth and dip values. **d**, Vollmer's trivariate fabric shape triangle[99]. **e**, Benn's fabric shape triangle[100].

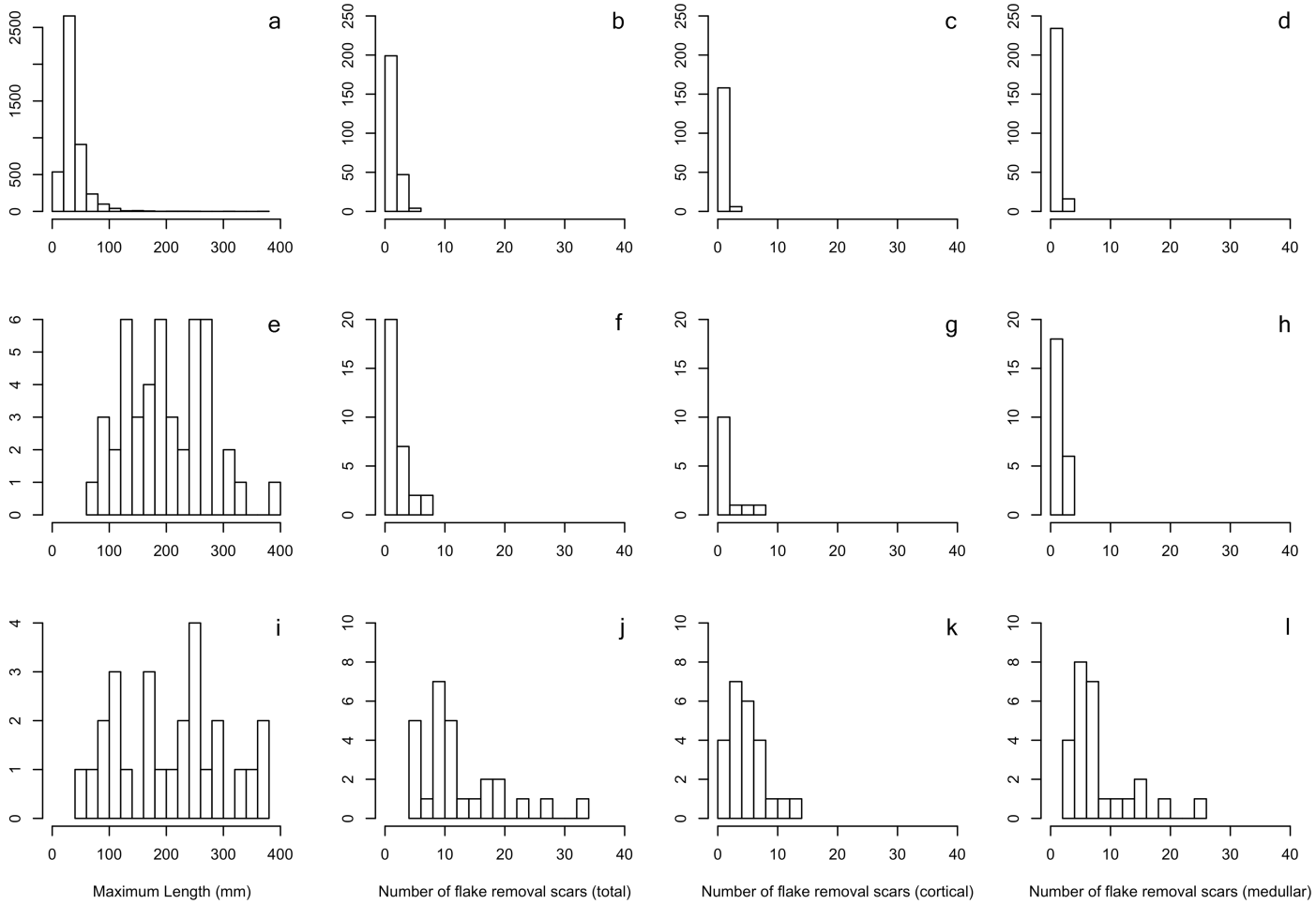

Extended Data Fig. 4 | Metric comparison (a,e,j) and number of flake removal scars (b-d, f-h, j-l) per specimens. Comparison of the maximum length between **a**, the bone fragments from the T69 Complex faunal assemblage, **e**, the diaphyseal fragment produced when fracturing elephant limb bones[4], and **i**, the bone fragments bearing flake removal scars interpreted as bone tools from the T69 Complex. The tools are considerably longer than the remainder of the faunal assemblage and fall within the size range of experimentally broken elephant long bones. Comparison of the number of flake removal scars per specimen between (**b**-**d**), a randomly selected sample of diaphyseal fragments from the T69 Complex faunal assemblage, (**f**-**h**) bone fragments produced during experimental bone fracturing to expose the marrow of horse[9] and elephant[4] limb bones, and (**j**-**l**) bone fragments bearing flake removal scars interpreted as tools from the T69 Complex. The total number of flake removal scars rarely exceed four in experimental settings (**f**) whether they are present on the cortical (**g**) or medullar aspect (**h**), which broadly matches the pattern observed for the comparative sample from the T69 faunal assemblage (**f**-**h**). Conversely, the bone tools from the T69 Complex display instead an average of 12.9 flake scars per specimen (**j**), preferentially arranged contiguously on both the cortical (**k**) and medullar (**l**) aspects.

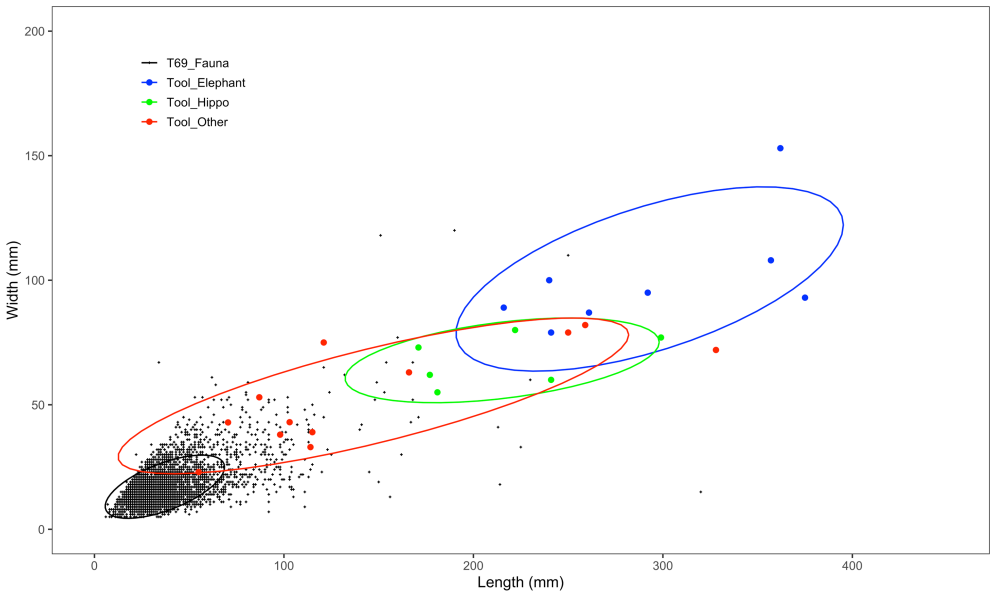

Extended Data Fig. 5 | Size comparison between the bone tools and the faunal assemblage from the T69 Complex. Scatterplot of the length and width of the bone fragments from the T69 Complex faunal assemblage (black) compared to those recorded for the bone tools made of elephant bones (blue), hippo bones (green), and bones from other or unidentified species (red). Part of that latter sample falls within the range of variability of both elephant and hippo as their cortical thickness suggests they originate from size 5 or 6 mammals (i.e., mammals weighting more than two tonnes). Confidence ellipses at 90%.

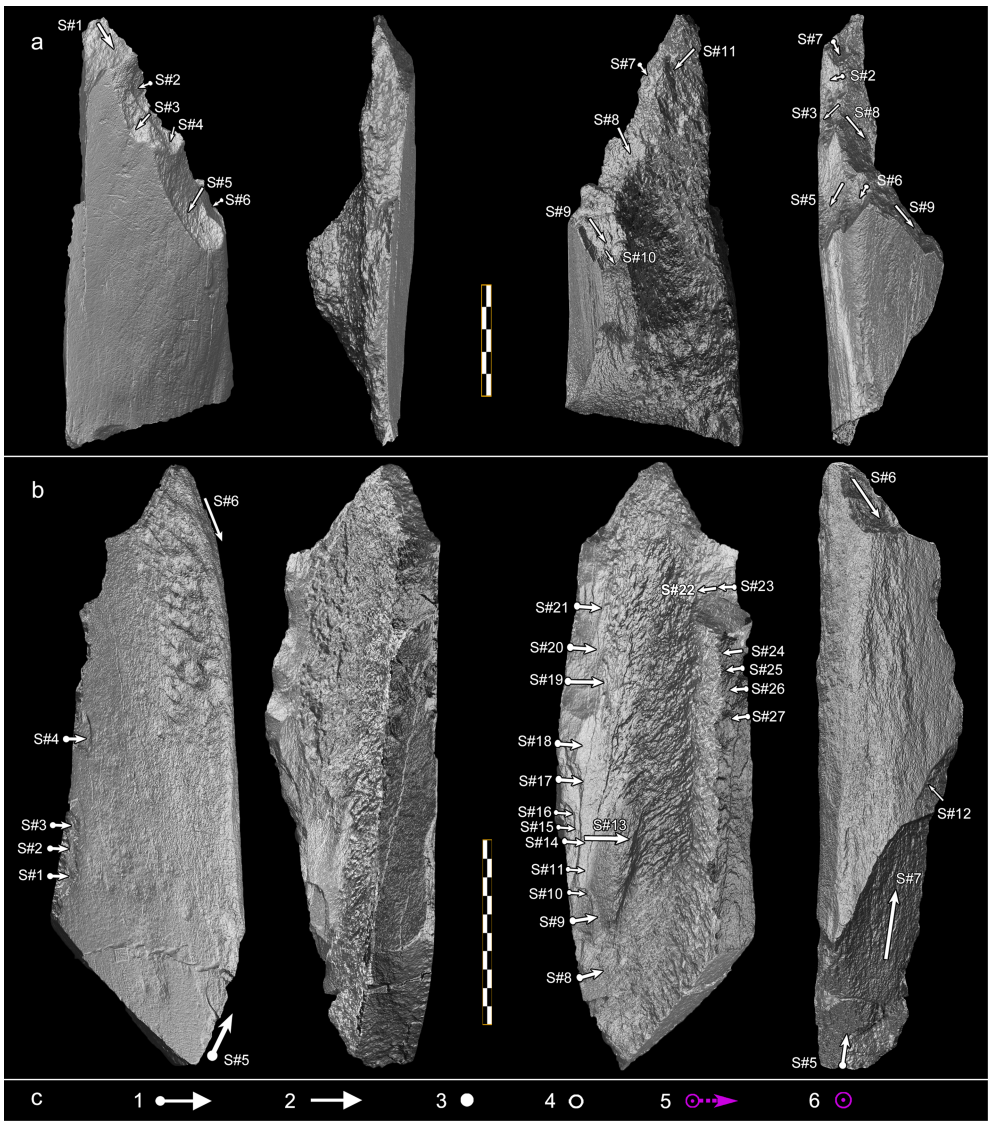

Extended Data Fig. 6 | 3D surface model images of bone tools. Illustrated in Fig. 1. **a**, Bifacially-flaked tool (accession number T69L20-3009; dimensions 166 × 63 × 44 mm). The left part (cortical aspect) is fractured, almost certainly after the distal end had already been shaped (as indicated by the truncated morphology of S#1). Order of flaking can be reconstructed in part (S#5 is offset by posterior S#6 and S#4; S#3 is partially erased by S#2), and indicates a recurrent sequence of shaping of the edges near the tip. **b**, Tool made of a proboscidean long bone fragment (accession number T79L10-2511; dimensions 292 × 95 × 66 mm). The scars on the medullar aspect are organized in two series of contiguous removals: the left edge series are struck from the cortical side and penetrate invasively into the cancellous tissue. In the right edge, S#24-27 were removed from a pre-existing fracture plane, thus indicating that the shaping took place after the bone shaft had been split. The distal end was fractured after shaping had occurred, as part of S#22 was removed by the tip fracture, and the edge where S#21 is located was also truncated by the fracture. The V-shaped angle of such fracture runs parallel to the tool axis, which is compatible with a percussive and compressive motion likely causing the tip breakage. Each scale bar segment, 1 cm. See also Supplementary Videos 4 and 5. **c**, Symbology (based on[101]): 1-Direction of flaking on scar with percussion point. 2- Direction of flaking on scar where percussion point is missing. 3- Percussion point of removal on the adjacent flaking surface. 4- Position of removal with absent percussion point on the adjacent flaking surface. 5- Striking direction on undetached flakes. 6- Percussion point of undetached flake on the adjacent flaking surface.

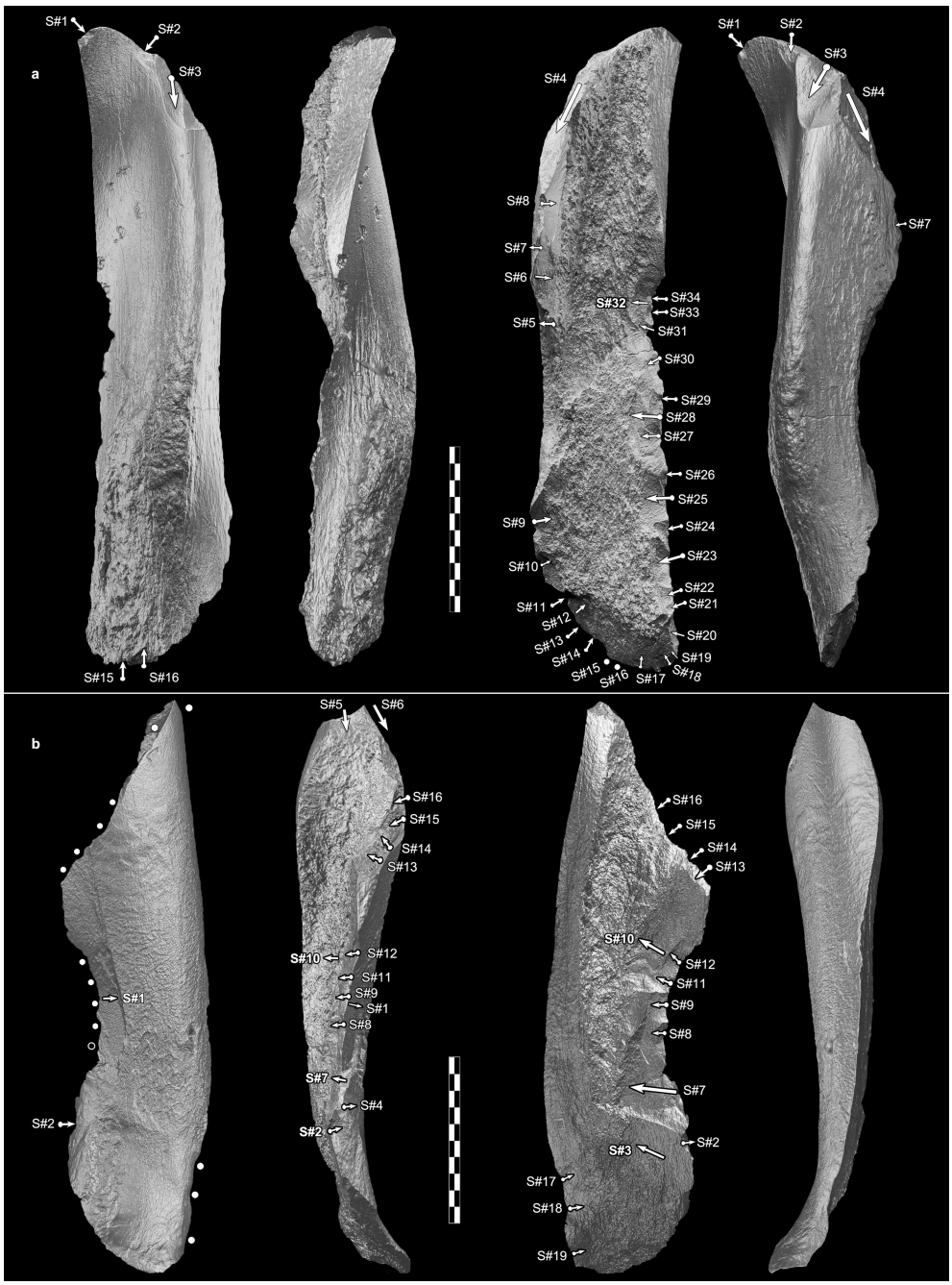

Extended Data Fig. 7 | Further 3D surface model images of bone tools. Illustrated in Fig. 3. These artefacts share similar techno-morphological features, in which the portion of long limb diaphysis closer to the epiphysis (where bones are thicker) is shaped into the tip of the tool, the base of the artefact is shaped in the portion near the metaphysis (thinner and with a more oval natural shape), and one lateral edge in the medial portion of the shaft is shaped into a deep notch. **a**, Massive tool made from the humerus of an elephant (accession number T79L10-9047; dimensions 375 × 93 × 105 mm). Series 1 (S#1-4): flake removals on the cortical aspect of the tip. Series 2 (S#5-8): sequence of alternating removals that indicates consecutive flipping of the blank. Series 3 (S#9-10): the cortical surface is used to strike flakes that are removed sequentially and clockwise. This series is truncated by (and hence is anterior to) the series starting with S#11. Series 4 (S#11-19): shaping of a crescent bottom at the base of the tool. Instead of wide and invasive removals such as those from the previous series, scars in Series 4 trim the edge to create a semicircular shape. Series 5 (S#20-29): unifacial removals from the cortical surface into the medullar side remove cancellous tissue and create a denticulate edge. Series 6 (S#30-34): a deep notch with several extractions within is created in the medial part of the edge. **b**, Unifacially-shaped bone tool (accession number T79L10-18461; dimensions 299 × 77 × 54 mm). Removals S#8-12 use scar S#1 as their percussion platform. Most of flaking is concentrated on one edge, where deep and invasive scars (S#3 and S#7) were succeeded by a contiguous sequence of flake removals aimed at creating a large notch (S#8-12) and shape the tip (S#13-16). Two V-shape scars (S#5-6) forming a dihedral angle at the tip run parallel to the tool axis are interpreted as fractures probably caused by percussive and compressive motions during tool use. Each scale bar segment, 1 cm. See additional details in Supplementary Videos 6 and 7.

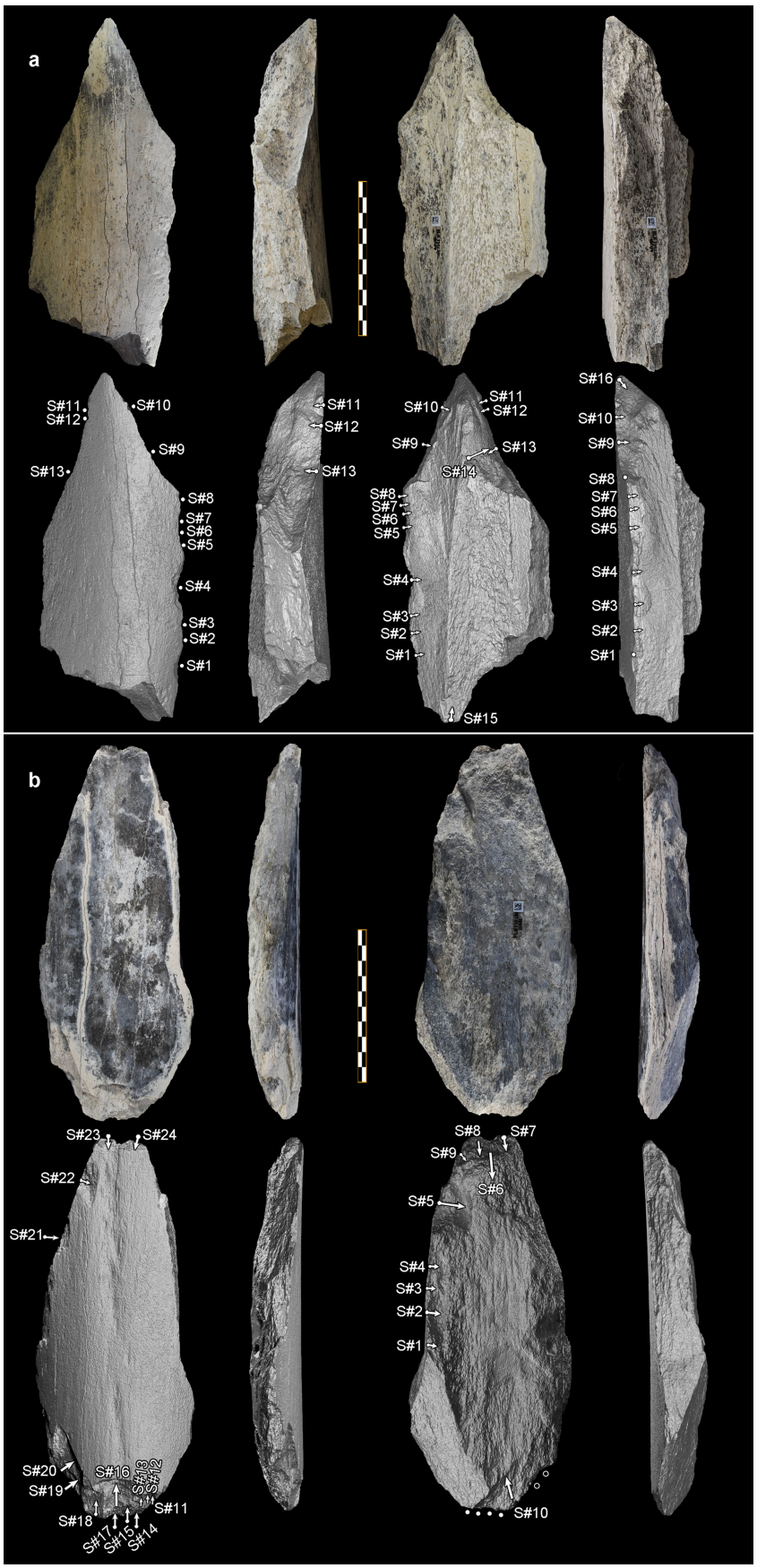

Extended Data Fig. 8 | See next page for caption.

Extended Data Fig. 8 | Additional examples of elephant bone artefacts. a, Unifacially-flaked bone tool (accession number T69L20-13007; dimensions 216 × 89 × 60 mm) on an indeterminable limb bone diaphyseal fragment. Bilateral removals on the distal part – S#9-10 on the right and S#11-13 on the left sides (cortical view)– shape a pointed end. Flake removals S#1-13 were struck from the cortical surface into pre-existing large fracture planes, and therefore occurred after the initial splitting of the diaphysis. Percussion points of most scars penetrate deep into the edge, producing large notches (e.g., S#1, S#4, S#6). **b**, Bifacially-flaked tool made on indeterminable diaphyseal fragment of limb bone (accession number T79L10-13631; dimensions 240 × 100 × 40 mm). Most scars on the medullar surface (S#1-5) used a pre-existing large fracture plane as the striking platform. Scar S#10 removes part of another pre-existing fracture plane, and is in turn largely obliterated by the S#11-20 flaking series. Removals on the proximal end (S#10-20) shape a crescent via recurrent flaking of the same area. Each scale bar segment, 1 cm.

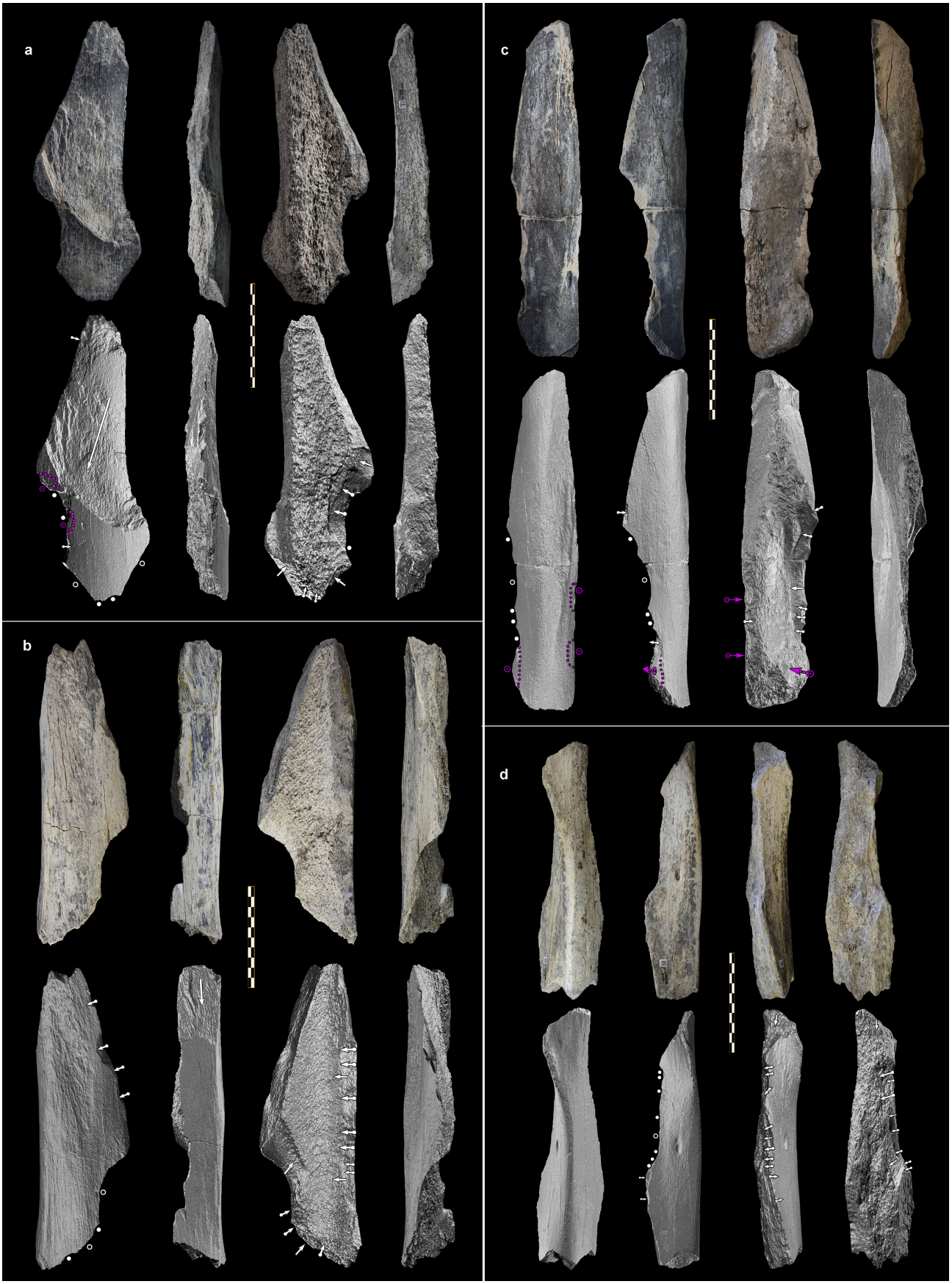

Extended Data Fig. 9 | See next page for caption.

Extended Data Fig. 9 | Additional examples of notched artefacts. **a**, Elephant long bone diaphysis (accession number T69L20-3633; dimensions 261 × 87 × 42 mm). **b**, Long bone diaphysis of size 5/6 mammal (accession number T77L64-823; dimensions 259 × 82 × 81 mm). **c**, Tibia diaphysis of size 5/6 mammal (accession number T69L20-6356; dimensions 328 × 72 × 68 mm). **d**, Humerus diaphysis of hippo (accession number T69L20-12450; dimensions 250 × 63 × 45 mm). Each scale bar segment, 1 cm.

Extended Data Fig. 10 | Remaining specimens in the T69 Complex bone tool assemblage. See accession numbers, skeletal, taxonomic and dimension data in Supplementary Data 2, and annotated flaking patterns in Supplementary Video 8. Each scale bar segment, 1 cm.

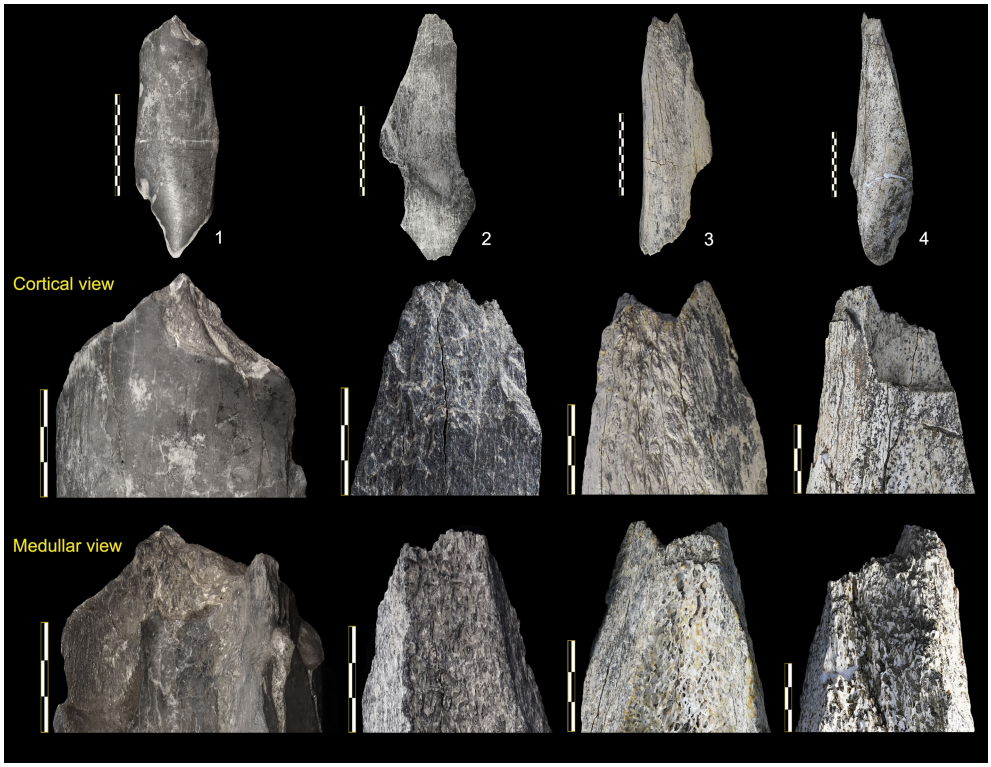

Extended Data Fig. 11 | Recurrent distal fracture patterns on additional bone tools. 1, Tibia diaphysis of cf. *Hippopotamus* (accession number T69L20-1872; dimensions 222 × 80 × 54 mm). 2, Accession number T69L20-3633 (see Extended Data Fig. 9a). 3, Accession number T77L64-823 (see Extended Data Fig. 9b). 4, Elephant long bone diaphysis (accession number T78L84-75; dimensions 353 × 103 × 53 mm). Each scale bar segment, 1 cm.

nature portfolio

Corresponding author(s): Ignacio de la Torre & Jackson K. Njau

Last updated by author(s): Dec 19, 2024

Reporting Summary

Nature Portfolio wishes to improve the reproducibility of the work that we publish. This form provides structure for consistency and transparency in reporting. For further information on Nature Portfolio policies, see our Editorial Policies and the Editorial Policy Checklist.

Statistics

For all statistical analyses, confirm that the following items are present in the figure legend, table legend, main text, or Methods section.

n/a	Confirmed	
☐	☒	The exact sample size (*n*) for each experimental group/condition, given as a discrete number and unit of measurement
☒	☐	A statement on whether measurements were taken from distinct samples or whether the same sample was measured repeatedly
☒	☐	The statistical test(s) used AND whether they are one- or two-sided *Only common tests should be described solely by name; describe more complex techniques in the Methods section.*
☒	☐	A description of all covariates tested
☒	☐	A description of any assumptions or corrections, such as tests of normality and adjustment for multiple comparisons
☒	☐	A full description of the statistical parameters including central tendency (e.g. means) or other basic estimates (e.g. regression coefficient) AND variation (e.g. standard deviation) or associated estimates of uncertainty (e.g. confidence intervals)
☐	☒	For null hypothesis testing, the test statistic (e.g. *F*, *t*, *r*) with confidence intervals, effect sizes, degrees of freedom and *P* value noted *Give P values as exact values whenever suitable.*
☒	☐	For Bayesian analysis, information on the choice of priors and Markov chain Monte Carlo settings
☒	☐	For hierarchical and complex designs, identification of the appropriate level for tests and full reporting of outcomes
☒	☐	Estimates of effect sizes (e.g. Cohen's *d*, Pearson's *r*), indicating how they were calculated

Our web collection on statistics for biologists contains articles on many of the points above.

Software and code

Policy information about availability of computer code

Data collection	ArcGIS Pro v. 3.3, R-Cran v. 4.4.1, Oriana v. 3.13
Data analysis	ArcGIS Pro 3.3, R-Cran v. 4.4.1, Oriana v. 3.13

For manuscripts utilizing custom algorithms or software that are central to the research but not yet described in published literature, software must be made available to editors and reviewers. We strongly encourage code deposition in a community repository (e.g. GitHub). See the Nature Portfolio guidelines for submitting code & software for further information.

Data

Policy information about availability of data

All manuscripts must include a data availability statement. This statement should provide the following information, where applicable:

- Accession codes, unique identifiers, or web links for publicly available datasets
- A description of any restrictions on data availability
- For clinical datasets or third party data, please ensure that the statement adheres to our policy

All data generated or analysed during this study are included in this published article and its supplementary information files.

Research involving human participants, their data, or biological material

Policy information about studies with human participants or human data. See also policy information about sex, gender (identity/presentation), and sexual orientation and race, ethnicity and racism.

Reporting on sex and gender	N/A
Reporting on race, ethnicity, or other socially relevant groupings	N/A
Population characteristics	N/A
Recruitment	N/A
Ethics oversight	N/A

Note that full information on the approval of the study protocol must also be provided in the manuscript.

Field-specific reporting

Please select the one below that is the best fit for your research. If you are not sure, read the appropriate sections before making your selection.

☒ Life sciences ☐ Behavioural & social sciences ☐ Ecological, evolutionary & environmental sciences

For a reference copy of the document with all sections, see nature.com/documents/nr-reporting-summary-flat.pdf

Life sciences study design

All studies must disclose on these points even when the disclosure is negative.

Sample size	The bone tool assemblage reported here contains 27 artefacts, derived from an archaeological horizon excavated across 295 square meters. This archaeological horizon also yielded abundant fossils (over 22,800 remains) from mammals, reptiles and fish, as well as over 10,900 stone tools larger than 2 cm. Mammal bones ≥2 cm (n = 8,930) were sampled for full zooarchaeological analysis. The sample selected for full zooarchaeological analysis (n = 2,075) included all items identified as bone tools, all proboscidian fossils (as these are particularly significant among the bone assemblage), and a sample from all other ≥2 cm mammal bone specimens. The archaeological bone tools were compared to: 1- Dimensions of a control sample (n = 4,507) of long bone fragments from the same archaeological excavation. 2- Features of flake removals in a sample (n = 250) of long bone fragments. 3-Published experimental samples of horse (Doyon et al., ref 9) and elephant (Backwell and d'Errico, ref. 4) long bones fractured to expose marrow.
Data exclusions	Due to the large size of the mammal assemblage, full zooarchaeological analysis was conducted in a sample of the determinable mammal fossils. This selection included all items identified as bone tools plus all proboscidean fossils, as well as a sample from all other determinable specimens. For the comparison of dimensions and flaking patterns between bone tools and the rest of the mammal assemblage from the T69 Complex, a control sample of the latter was selected (see details in Methods).
Replication	All bones tools were first-hand analysed by two pairs of co-authors (IdlT-JKN and LD-Fd'E), and then each artefact was discussed in group meetings during two separate sessions of several days each, approximately 1 year apart. Results are available in Supplementary Information Dataset 2, which contains all data collected from each item interpreted as a bone tool. Each item is labelled with a unique ID that will enable reproducibility of data collection for any researcher re-studying the assemblage.
Randomization	Horizontal spatial distribution of all archaeological was tested through an Average Nearest Neighbour Analysis that compared the actual distance between items to a hypothetical random sample, following Ebdon (ref. 57).
Blinding	Bone tools were independently analysed by IdlT and LD-Fd'E, after which specimen features were discussed as a group and recorded in Supplementary Information Dataset 2.

Reporting for specific materials, systems and methods

We require information from authors about some types of materials, experimental systems and methods used in many studies. Here, indicate whether each material, system or method listed is relevant to your study. If you are not sure if a list item applies to your research, read the appropriate section before selecting a response.

Materials & experimental systems

n/a	Involved in the study
☒	☐ Antibodies
☒	☐ Eukaryotic cell lines
☐	☒ Palaeontology and archaeology
☒	☐ Animals and other organisms
☒	☐ Clinical data
☒	☐ Dual use research of concern
☒	☐ Plants

Methods

n/a	Involved in the study
☒	☐ ChIP-seq
☒	☐ Flow cytometry
☒	☐ MRI-based neuroimaging

Palaeontology and Archaeology

Specimen provenance	All specimens are derived from excavations directed by at the FLK West T69 Complex in Olduvai Gorge. Fieldwork permits were renewed annually by the Tanzanian Commission for Science and Technology (COSTECH), the Ngorongoro Conservation Authority Area (NCAA), and the Department of Antiquities, Tanzanian Ministry of Natural Resources and Tourism, and an export permit for analysis was granted by the Department of Antiquities.
Specimen deposition	The specimens will be permanently housed at the Olduvai Research Laboratory in the Leakey Camp, a research and storage facility managed by the Tanzanian Ministry of Natural Resources and Tourism.
Dating methods	No new dates are provided

☐ Tick this box to confirm that the raw and calibrated dates are available in the paper or in Supplementary Information.

Ethics oversight	Fieldwork and analysis protocols abided by guidance provided by COSTECH, NCAA, and the Department of Antiquities, Tanzanian Ministry of Natural Resources and Tourism.

Note that full information on the approval of the study protocol must also be provided in the manuscript.

Plants

Seed stocks	*Report on the source of all seed stocks or other plant material used. If applicable, state the seed stock centre and catalogue number. If plant specimens were collected from the field, describe the collection location, date and sampling procedures.*
Novel plant genotypes	*Describe the methods by which all novel plant genotypes were produced. This includes those generated by transgenic approaches, gene editing, chemical/radiation-based mutagenesis and hybridization. For transgenic lines, describe the transformation method, the number of independent lines analyzed and the generation upon which experiments were performed. For gene-edited lines, describe the editor used, the endogenous sequence targeted for editing, the targeting guide RNA sequence (if applicable) and how the editor was applied.*
Authentication	*Describe any authentication procedures for each seed stock used or novel genotype generated. Describe any experiments used to assess the effect of a mutation and, where applicable, how potential secondary effects (e.g. second site T-DNA insertions, mosiacism, off-target gene editing) were examined.*